TRPA1 activation in a human sensory neuronal model: Relevance to cough hypersensitivity?

TRPA1 activation in a human sensory neuronal model: Relevance to cough hypersensitivity?

Rebecca Clarke PhD[a], Kevin Monaghan PhD[a], Imad About, PhD[b], Caoimhin S. Griffin, BSc[c], Gerard P. Sergeant, PhD[c], Ikhlas El Karim, PhD[a], J. Graham McGeown PhD[a], S. Louise Cosby PhD[a], Timothy M. Curtis PhD[a], Lorcan P. McGarvey MD[a]*, Fionnuala T. Lundy PhD[a*].

[a]Centre for Experimental Medicine, Wellcome-Wolfson Institute for Experimental Medicine, School of Medicine, Dentistry and Biomedical Sciences, Queen's University, Belfast, Northern Ireland

[b]Aix Marseille Université, CNRS, ISM UMR 7287, 13288, Marseille, France

[3]Smooth Muscle Research Centre, Dundalk Institute of Technology, Dundalk, Co. Louth, Ireland

*denotes joint senior authorship

Correspondence
Dr Lorcan McGarvey
Centre for Experimental Medicine
Wellcome-Wolfson Institute for Experimental Medicine
School of Medicine, Dentistry and Biomedical Sciences
97 Lisburn Road
Belfast
BT9 7BL
l.mcgarvey@qub.ac.uk

FUNDING

This work was funded by the National Centre for the Replacement, Refinement and Reduction of Animals in Research (NC3Rs) and the Pain Relief Foundation (UK).

ABSTRACT

The cough reflex becomes hyper-responsive in acute and chronic respiratory diseases, but understanding the underlying mechanism is hampered by difficulty accessing human tissue containing both nerve endings and neuronal cell bodies. We refined an adult stem-cell sensory neuronal model to overcome the limited availability of human neurones and applied the model to study transient receptor potential ankyrin 1 (TRPA1) channel expression and activation.

Human dental pulp stem cells (hDPSCs) were differentiated towards a neuronal phenotype, termed peripheral neuronal equivalents (PNEs). Using molecular and immunohistochemical techniques, together with Ca^{2+} microfluorimetry and whole cell patch clamping, we investigated roles for nerve growth factor (NGF) and the viral mimic Poly I:C in TRPA1 activation.

PNEs exhibited morphological, molecular and functional characteristics of sensory neurons and expressed functional TRPA1 channels. PNE treatment with NGF for 20 minutes generated significantly larger inward and outward currents compared to untreated PNEs in response to the TRPA1 agonist, cinnamaldehyde ($p<0.05$). PNE treatment with Poly I:C caused similar transient heightened responses to TRPA1 activation compared to untreated cells.

Using the PNE neuronal model we observed both NGF and Poly I:C mediated sensory neuronal hyper-responsiveness, representing potential neuro-inflammatory mechanisms associated with heightened nociceptive responses recognised in cough hypersensitivity syndrome.

Take home message

Development of a novel human adult stem cell neuronal model to investigate neural hyper-responsiveness in cough

INTRODUCTION

Airway sensory nerves control cough and represent a means by which the lung clears secretions and protects itself against inhaled foreign bodies and irritants[1]. In conditions such as asthma and chronic cough this neural reflex becomes hyper-responsive causing troublesome bouts of cough typically triggered by low level physical and chemical stimuli[2, 3]. These abnormal sensory responses often worsen during respiratory viral infections and while the effects of virus on airway epithelial and immune cells has been extensively studied little is known regarding the mechanisms responsible for airway neural hyper-responsiveness[4-6]. Although the symptoms associated with airway hyper-responsiveness are what disturb patients most about their condition, there are no current treatments that adequately alleviate and 'reset' this state[7]. Potential therapeutic targets include the transient receptor potential (TRP) cation channels which are responsible for sensing chemical and physical stimuli and are expressed on many cell types including airway sensory nerves[8]. We have previously shown that human rhinovirus upregulates expression of TRP ankyrin 1 (TRPA1) and TRP vanilloid 1 (TRPV1) channels in a neuronally differentiated immortalized human neuroblastoma cell line[9], however the mechanisms involved in nerve hyper-responsiveness remain to be investigated.

A number of neuroactive molecules are released into the airway following respiratory viral infection including nerve growth factor (NGF) which alters TRP channel function[10] and may be important in regulating airway sensory nerve responsiveness. In addition, sensory neurons are known to express Toll-like receptors (TLRs) which play a key role in host defence during microbial infection[11]. Toll-like receptor 3 (TLR 3) is of particular interest as it responds to viral double-stranded RNA (dsRNA), a by-product of replicating viruses including rhinovirus[12] and represents a potential route through which viral infection may induce cough reflex hyper-responsiveness.

Investigating TRP channel expression and regulation in human sensory neurons is challenging because the cell bodies of peripheral neurons are housed in neuronal ganglia which are not accessible by biopsy. Although TRP channel studies have been conducted in animal models[13-15] there are recognised interspecies differences in TRP function and expression[16-18]. Furthermore, in light of EU legislation for the protection of animals for scientific purposes there is an urgent need for development of a new generation of *in vitro* models based on human biology[19]. Thus, a human neuronal model could complement or potentially replace some animal models currently used in respiratory research and provide data that is relevant to human physiology.

Dental pulp tissue derives from migrating neural crest cells during development[20,21] and is a source of multipotential stem/progenitor cells. The propensity for human dental pulp stem cells (hDPSCs) to differentiate towards a neuronal phenotype, previously termed peripheral neuronal equivalents (PNEs), has been reported[22-24] and is likely to be explained by their neural crest origin. Neural crest stem cells are the main contributors to the development of peripheral nerve fibres, including those of the trigeminal ganglion of the trigeminal nerve[25, 26] and jugular ganglion of the vagus nerve[27]. Jugular ganglion C-fibres terminate within the extrapulmonary airways and respond directly to tussive stimuli such as capsaicin and bradykinin, express neuropeptides and tachykinins, and are thus considered important in nociceptive airway responses such as cough. Here we describe the development of a functional human *in vitro* neuronal model differentiated from hDPSCs, suitable for studying the role of neuroinflammatory factors in TRPA1 channel-mediated neuronal hyper-responsiveness.

Methods

Full details are available in the online supplement.

Cell culture and hDPSC enrichment

Human dental pulp cells were harvested from immature permanent third molar teeth in accordance with French ethics legislation[28] and maintained in minimal essential medium-alpha (MEM-alpha) supplemented with 10% fetal bovine serum (FBS), 100 UI/mL penicillin and 100 µg/mL streptomycin, L-glutamine and 200 µM ascorbic acid. hDPSCs were enriched in dental pulp cell cultures by preferential adhesion to fibronectin (10 µg/mL overnight at 4°C) coated 6-well plates and incubated at 37°C for 20 minutes. Non-adherent cells were discarded. hDPSCs were maintained on fibronectin for 2 days in MEM-alpha.

Neural Induction

hDPSCs were harvested from fibronectin-coated plates using trypsin and seeded onto plastic/glassware coated with poly-l-ornithine (0.01%) and laminin (5 µg/ml) and incubated with neurobasal A supplemented with B27, glutaMAX, human basic fibroblast growth factor (40 ng/mL) and epithelial growth factor (40 ng/ml) for 7 days.

Immunofluorescence

PNEs were differentiated from hDPSCs as described above on circular coverslips (16 mm, thickness 1). Cells were washed in phosphate buffered saline (PBS) and fixed by submerging in ice cold acetone for 8 minutes then air dried. Cells were washed in PBS and blocked for non-specific binding by incubation with 10% normal goat serum.

Cells were treated with specific primary antibody (Table S1; in 10% goat serum) overnight at 4°C. Appropriate anti-species Alexa Fluor secondary antibody conjugates were diluted in PBS containing 0.1% Triton X 100 and applied to cells for 1h at room temperature. Samples were mounted using ProLong Gold with DAPI and viewed using a fluorescent microscope.

qRT-PCR

Neural induction of hDPSCs towards PNEs was achieved as outlined above except that cells were grown in 96 well plates. Total RNA was harvested using the PicoPure RNA isolation kit and quantified using a Take3 plate and plate reader. RNA samples were reverse transcribed using the SuperScript VILO cDNA synthesis kit according to the manufacturer's instructions. qPCR reactions were set up using TaqMan universal mastermix with UNG according to the manufacturer's instructions using predesigned Taqman primers (Table S2, S3). qPCR was carried out using the Stratagene PCR instrument and analysed using Mx3005P software.

Whole Cell Patch Clamp

PNEs were differentiated as described on coverslips (thickness 0). Whole cell currents were recorded using borosilicate patch pipettes (2 – 5 MΩ resistance), an Axopatch 200B amplifier and pClamp9 software.

To measure voltage-gated Na+ channel activity, CsCl bath (150 mM NaCl, 6 mM CsCl, 1 mM MgCl2, 1.5 mM CaCl2, 5 mM glucose and 10 mM HEPES in dH2O. pH altered to 7.4 using Tris) and pipette (120 mM CsCl, 1 mM MgCl2, 4 mM Na2ATP, 10 mM BAPTA and 10 mM HEPES in dH2O. pH altered to 7.2 using Tris) solutions were used. 1 µM tetrodotoxin (TTX) was made up in CsCl bath solution. Experiments were carried out at room

temperature. The holding potential was -120 mV. Current-voltage (I-V) relationships were measured using a voltage step protocol.

TRP channel activity was recorded using a CsCl bath solution and a Cs-aspartate pipette solution (100 mM CsOH.2H2O, 100 mM aspartic acid, 20 mM CsCl, 1 mM MgCl2, 4 mM Na2ATP, 0.08 mM CaCl2, 10 mM BAPTA and 10 mM HEPES in dH2O. pH altered to 7.2 using Tris). 100 µM cinnamaldehyde, 10 µM HC030031, 10 µM capsaicin and 20 µM capsazepine were made up in CsCl bath solution. Experiments were carried out at 37°C. The holding potential was 0 mV throughout. I-V relationships were recorded using a voltage ramp protocol. All data were analysed using Clampfit9 software.

Microfluorimetric Calcium Imaging

For microfluorimetric calcium imaging PNEs were differentiated as described on coverslips (thickness 0). PNEs were loaded with Fura-2AM (5 µM) for 40 minutes at 37°C, placed into a recording chamber mounted on the stage of an inverted microscope and superfused with hanks (140 mM NaCl, 5 mM KCl, 2 mM CaCl2.2H2O, 1 mM MgCl2, 10 mM HEPES free acid and 5 mM glucose in dH2O. pH altered to 7.4 using NaOH). All solutions were kept at a 37°C using a water bath and perfusion system. [Ca2+]i was measured (details in online supplement) and TRP channel activity was observed as changes in [Ca2+]i following stimulation with 10 µM capsaicin and 10 µM capsazepine diluted in Hanks.

Confocal Ca2+ imaging

PNEs were loaded with 0.4µM fluo-4/AM for 6 minutes at room temperature and imaged using an iXon887 EMCCD camera (Andor Technology, Belfast) coupled to a Nipkow

spinning disk confocal head (CSU22, Yokogawa, Japan). A krypton-argon laser (Melles Griot UK) at 488 nm was used to excite the fluo-4, and the emitted light was detected at wavelengths >510 nm. Experiments were performed using a x60 objective (Olympus) and images were acquired at 15 frames per second. Background fluorescence from the camera, obtained using a null frame, was subtracted from each frame to obtain 'F'. F0 was determined as the minimum fluorescence under control conditions. The pseudo line-scan image and corresponding intensity profile plot (Figs 2D,E) were obtained using Image J software (NIH). ΔF/F0 refers to the measurement of the change in Ca2+ levels from basal to peak.

ELISA

PNEs were differentiated in 96 well plates. Supernatants were collected following treatments (as outlined below) and IL8 and IL6 levels were measured using human IL8 and IL6 DuoSet ELISA kits (R&D) according to the manufacturer's instructions.

Treatment of PNEs

PNEs were treated with pro-inflammatory cytokines (nerve growth factor (NGF; 100 ng/ml); interleukin 1β (IL1β; 5 ng/ml); tumour necrosis factor alpha (TNFα; 10 ng/ml)) and Poly I:C (2 μg/ml) for 20 minutes, 6h or 24h(Table S4). Control cells were incubated with medium alone.

Results

Enriched hDPSCs undergo neuronal differentiation to become functional PNEs

hDPSCs expressed the neural crest protein markers, P75, AP2α and HNK1 (Fig. S1) and displayed a fibroblastic morphology consisting of splayed multipolar elongations (Fig. 1A). Following 7 days neuronal differentiation, cells acquired a typical bipolar neuronal morphology with a centrally located swollen cell body and axon-like projections (Fig. 1B). Immunofluorescence confirmed a phenotype change from hDPSC to PNE during differentiation, manifest by loss of expression of the fibroblast marker FSP (Fig 1C, D) and gain of specific mature neuronal markers PGP9.5 (Fig. 1E, F) and synaptophysin (Fig. 1G, H). PNEs also expressed the neuropeptides substance P and CGRP, consistent with a sensory neuronal phenotype (Fig. S2).

Using whole cell patch clamping the neuronal phenotype of PNEs was further confirmed by demonstrating functional voltage-gated Na^+ (NaV) channels. Using Cs-based bath and pipette solutions to block outward K^+ currents, a family of rapidly inactivating inward currents were consistently generated when a series of 500 ms depolarising voltage steps were applied in 5 mV increments from an initial holding potential of -120 mV (Fig. 1I) to a final test potential of 55 mV. Currents were completely inhibited by the Na^+ channel inhibitor, TTX (1 μM) (Fig. 1J). Currents, normalised against cell capacitance, were plotted to show the I-V relationship (Fig. 1K).

Since TRPV1 has long been associated with a neuronal phenotype, its gene and protein expression in PNEs was determined by qPCR (Table S5) and immunofluorescene (Fig 1L). To confirm TRPV1 functionality in PNEs, whole cell patch clamping was performed using Cs^+-based bath and pipette solutions. Using a voltage ramp protocol, significant increases in both inward and outward currents were observed following application of the TRPV1 agonist

capsaicin (10 μM), which were significantly inhibited by capsazepine (20 μM; Fig. 1M, N). Vehicle only controls were unresponsive (Fig S3). To further confirm the suitability of PNEs for functional studies, microfluorimetric $[Ca^{2+}]_i$ imaging was performed for TRPV1 activity. Fura-loaded PNEs were shown to demonstrate spontaneous activity (Fig. S4), a characteristic of functional neurons, and upon capsaicin application an instantaneous increase in PNE $[Ca^{2+}]_i$ was observed (Fig. S5A), with $[Ca^{2+}]_i$ levels falling immediately afterwards. In the presence of the TRPV1 antagonist, capsazepine, PNE $[Ca^{2+}]_i$ did not increase above basal levels (Fig. S5B). The change in ratio with capsaicin in the absence and presence of capsazepine was graphed for statistical analysis (Fig. S5C).

PNEs express functional TRPA1

Having established the neuronal phenotype of PNEs (Fig. 1) their suitability for studying TRPA1 channels was investigated. TRPA1 gene expression was confirmed by qPCR (Table S5) along with protein expression by immunofluorescence (Fig. 2A). To study the functional TRPA1 on PNEs, whole cell patch clamp experiments were performed using Cs^+-based bath and pipette solutions. Using a voltage ramp protocol, significant increases in both inward and outward currents were observed in PNEs following application of cinnamaldehyde (100 μM) which were blocked by HC030031 (10 μM; Fig 2B,C). Vehicle only controls were unresponsive (Fig S3). To further confirm the suitability of PNEs for functional TRPA1 studies we examined the effect of cinnamaldehyde (100 μM) on Ca^{2+} levels in single PNEs using confocal Ca^{2+} imaging. Cinnamaldehyde induced robust rises in $[Ca^{2+}]_i$ that were reversibly inhibited by subsequent HC030031 application (see representative Figs. 2D,E and summary plot in Fig. 2F, n=9). Cinnamaldehyde responses were demonstrated to be concentration dependent (Figs 2G&H), with an EC_{50} of 54 μM. Using microfluorimetric

$[Ca^{2+}]_i$ imaging fura-loaded PNEs showed spontaneous activity (Fig. S4), and upon application of cinnamaldehyde an instantaneous increase in PNE $[Ca^{2+}]_i$ was observed (Fig. S6A), followed by falling $[Ca^{2+}]_i$ levels immediately afterwards. In the presenceHC030031, PNE $[Ca^{2+}]_i$ did not increase above basal levels (Fig. S6B). The mean change in ratio was graphed for statistical analysis (Fig. S6C).

NGF induces TRPA1 hyper-responsiveness on PNEs

NGF is known to induce hyper-responsiveness in sensory neurons [10, 29, 30] and is therefore a neuropathic cytokine worthy of investigating in this *in vitro* model. PNEs treated with NGF for 20 minutes immediately prior to patch clamp experiments generated significantly ($p < 0.05$) larger inward and outward currents when stimulated with cinnamaldehyde (Fig. 3A), demonstrating that PNE TRPA1 channels hyper-responsiveness in the presence of NGF. This hyper-responsive state was not sustained as PNEs treated for 24h did not generate the larger currents observed previously (Fig. 3A).

To investigate whether TRPA1 gene expression was altered following NGF treatment we undertook qRT-PCR on PNEs incubated with NGF for 6h and 24h. No significant changes in TRPA1 gene expression were observed (Fig. 3B). To determine whether this was an NGF-specific effect, we treated PNEs with the proinflammatory cytokines TNFα (10 ng/ml) and IL1β (5 ng/ml), and observed no significant change in TRPA1 gene expression (Fig. S7).

We also investigated whether similar effects in response to NGF treatment were observed in PNEs stimulated with capsaicin. No significant changes in capsaicin-induced currents were seen between untreated and NGF treated cells (Fig. S8A). Similarly, no changes were determined in TRPV1 gene expression following NGF treatment (Fig. S8B).

The viral mimetic Poly I:C induces IL8 release and TRPA1 hyper-responsiveness in PNEs

Poly I:C was employed to demonstrate the usefulness of the model to investigate the effects of viral infections on sensory neurons. Cell supernatants from PNEs incubated with Poly I:C were analysed for IL8 and IL6. Supernatants from control cells, and those incubated with Poly I:C for 6h showed no significant change in IL8 levels, and no detectable IL6 in controls (Fig. 4A, B). However, supernatants from cells incubated with Poly I:C for 24h had significantly higher levels of IL8 (2140.8 pg/ml) and IL6 (246.5 pg/ml) (Fig. 4A, B). Additional concentration and time-dependent effects of Poly I:C on IL8 levels are reported in Fig S9.

Poly I:C also induced TRPA1 hyper-responsiveness in PNEs. Treatment of PNEs with Poly I:C for 20 minutes immediately prior to patch clamping generated significantly larger inward and outward currents in response to cinnamaldehyde, compared with untreated PNEs (Fig. 4C). PNEs incubated with Poly I:C for 24h were not readily amenable to patch-clamp recording, suggesting changes had occurred in the plasma membrane. No significant changes were observed in TRPA1 gene expression following 6h or 24h Poly I:C treatments (Fig. 4D).

Discussion

In this study we successfully differentiated stem cells from human dental pulp towards PNEs which have morphological, molecular and functional characteristics of sensory neurons. We observed TRPA1 channel hyper-responsiveness following stimulation with both NGF and the viral mimic Poly I:C. Responses were rapid in onset, and independent of TRPA1 gene expression. Taken together our data suggest that PNEs represent a novel, species-specific *in vitro* model for the investigation of TRPA1 channel function and regulation on human

sensory neurons. We believe this model has potential to provide insight into the potential mechanisms involved in cough hypersensitivity.

An important refinement in our approach was the enrichment of hDPSCs from dental pulp cultures using differential fibronectin adhesion, allowing a phenotype switch from hDPSC to PNE in 7 days compared with 21 days previously reported using dental pulp cell cultures [22]. Functional neuronal activity in differentiated cells as described herein, should be considered a prerequisite for neuronal characterisation, particularly in view of the finding that voltage-dependent sodium channels are not present on hDPSCs[31].

To provide evidence for the suitability of PNEs as an *in vitro* model for the study of inflammatory TRP channel regulation we investigated the effect of the neurotrophic cytokine NGF. Levels of NGF are elevated in the airways of asthmatics[32] and in children with influenza infection airway NGF levels are increased and correlate with disease severity and cough duration[33] We observed that NGF rapidly induced increased TRPA1 activation consistent with that reported previously in primary cultures of mouse sensory neurons[28]. Such rapid effects are likely to be due to activation of intracellular cell signalling pathways resulting in phosphorylation of the TRP channel with subsequent channel hyper-responsiveness[9]. Our data suggest NGF can rapidly induce TRPA1 channel hyper-responsiveness, supporting a role for transcription-independent mechanisms in regulating TRP responses[10]. Interestingly, we did not see increased responses to capsaicin in NGF-treated cells, previously reported in a guinea pig model *in vivo*[34]. This disparity could serve to highlight differences between animal and human tissues and may add clinical relevance to the PNE model. It is also notable that positive preclinical data in animal models of the

TRPV1 antagonist XEN-D0501 sharply contrasts the lack of efficacy reported in a placebo controlled trial in chronic cough[35].

Following PNE treatment with the viral mimic Poly I:C significant increases in IL8 and IL6 secretion and increased currents in response to cinnamaldehyde, were observed compared to untreated PNEs. This is the first report to suggest a functional relationship between TRPA1 and Poly I:C. It is known that the viral mimetic Poly I:C mimics the pathogen associated molecular pattern (PAMP) dsRNA, and activates three pattern recognition receptors (PRRs) TLR3, retinoic acid-inducible gene 1 (RIG-I) and melanoma differentiation-associated protein 5 (MDA5)[36]. Functional interactionsTRPA1 and Poly I:C could therefore be mediated *via* one or more of these receptors.

In conclusion, PNEs represent a novel species-specific *in vitro* model suitable for the study of TRP channel function and regulation on human sensory neurons which is in line with current EU and UK directives to replace, reduce and refine the use of animals in research[19]. Using this model we have demonstrated that NGF and the viral mimic Poly I:C directly and rapidly induce a TRP channel hyper-responsiveness on the cell membranes of human sensory nerves representing a possible neuro-inflammatory process responsible for cough reflex hyper-responsiveness. We have been careful to distinguish our experimental findings of neuronal hyper-responsiveness from neuronal hypersensitivity. Under experimental neuro-inflammatory conditions we observed an increased neural response for a given stimulus which may have a clinical parallel in the form of ‘hypertussia’ observed in patients with Cough Hypersensitivity Syndrome (CHS) [37]. We have yet to determine if our PNE model can be rendered ‘hypersensitive’ to low level stimulation. CHS is a disorder gaining increasing recognition amongst respiratory, allergy, gastroenterology, speech/voice and otolaryngology healthcare professionals[37]. There is a need to improve our understanding of the neurobiology of this condition and we believe the novel techniques we report in this

manuscript and the clinical relevance of our experimental findings will be of interest to those working in this field.

Acknowledgements

We acknowledge the skilful technical assistance of Catherine Fulton.

REFERENCES

1 Canning BJ, Chang AB, Bolser DC, et al. Anatomy and neurophysiology of cough: CHEST Guideline and Expert Panel report. Chest 2014;**146**:1633-1648.

2 Chung KF, McGarvey L, Mazzone SB. Chronic cough as a neuropathic disorder. Lancet Respir Med. 2013;**1**(5):414-22.

3 Morice AH, Millqvist E, Belvisi MG, et al. Expert opinion on the cough hypersensitivity syndrome in respiratory medicine. Eur Respir J. 2014;44(5):1132-48

4 McErlean P, Favoreto S Jr, Costa FF, et al. Human rhinovirus infection causes different DNA methylation changes in nasal epithelial cells from healthy and asthmatic subjects. BMC Med Genomics 2014;**7**.

5 Patel DA, You Y, Huang G, et al. Interferon response and respiratory virus control are preserved in bronchial epithelial cells in asthma. J Allergy Clin Immunol 2014;**134**:1402-1412.

6 Guo H, Baker SF, Martinez-Sobrido L, et al. Induction of CD8 T cell heterologous protection by a single dose of single-cycle infectious influenza virus. J Virol 2014;**88**:12006-12016.

7 McGarvey L, McKeagney P, Polley L, et al. Are there clinical features of a sensitized cough reflex? Pulm Pharmacol Ther 2009;**22**:59-64.

8 Bessac BF, Jordt SE. Breathtaking TRP channels: TRPA1 and TRPV1 in airway chemosensation and reflex control. Physiology 2008;**23**:360-370.

9 Abdullah H, Heaney LG, Cosby SL, et al. Rhinovirus upregulates transient receptor potential channels in a human neuronal cell line: implications for respiratory virus-induced cough reflex sensitivity. Thorax 2014;**69**:46-54.

10 Ji RR, Samad TA, Jin SX, et al. p38 MAPK activation by NGF in primary sensory neurons after inflammation increases TRPV1 levels and maintains heat hyperalgesia. Neuron 2002;**36**:57-68.

11 Lafon M, Megret F, Lafage M, et al. The innate immune facet of brain: human neurons express TLR3 and sense viral dsRNA. J Mol Neurosci 2006;**29**:184-194.

12 Jacobs BL, Langland JO. When two strands are better than one: the mediators and modulators of the cellular responses to double-stranded RNA. Virology 1996;**219**:339-349.

13 Honore P, Chandran P, Hernandez G, et al. Repeated dosing of ABT-102, a potent and selective TRPV1 antagonist, enhances TRPV1-mediated analgesic activity in rodents, but attenuates antagonist-induced hyperthermia. Pain 2009;**142**:27-35.

14 Malek S, Sample SJ, Schwartz Z, et al. Effect of analgesic therapy on clinical outcome measures in a randomized controlled trial using client-owned dogs with hip osteoarthritis. BMC Vet Res 2012;**8**.

15 de la Roche J, Eberhardt MJ, Klinger AB, et al. The molecular basis for species-species activation of human TRPA1 protein by protons involves poorly conserved residues within transmembrane domains 5 and 6. J Biol Chem 2013;**288**:20280-20292.

16 Jordt SE, Julius D. Molecular basis for species-specific sensitivity to "hot" chilli peppers. Cell 2002;**108**:421-430.

17 Klionsky L, Tamir R, Gao B, et al. Species-specific pharmacology of Trichloro(sulfanyl)ethyl benzamides as transient receptor potential ankyrin 1 (TRPA1) antagonists. Mol Pain 2007;**3**.

18 Bianchi BR, Zhang XF, Reilly RM, et al. Species comparison and pharmacological characterization of human, monkey, rat, and mouse TRPA1 channels. J Phatmacol Exp Ther 2012;**341**:360-368.

19 European Commission Directive 2010/63/EU. Legislation for the protection of animals used for scientific purposes.

20 d'Aquino R, De Rosa A, Laino G, et al. Human dental pulp stem cells: from biology to clinical applications. J Exp Zool B Mol Dev Evol 2009;**312B**:408-415.

21 Coura GS, Garcez RC, de Aquiar CB, et al. Human periodontal ligament: a niche of neural crest stem cells. J Periodontal Res 2008;**43**:531-536.

22 Arthur A, Rychkov G, Shi S, et al. Adult human dental pulp stem cells differentiate toward functionally active neurons under appropriate environmental cues. Stem Cells 2008;**26**:1787-1795.

23 Urraca N, Memon R, El-Iyachi I, et al. Characterization of neurons from immortalized dental pulp stem cells for the study of neurogenetic disorders. Stem Cell Res. 2015 Nov;15(3):722-30.

24 Ullah I, Subbarao RB, Kim EJ, Bharti D, Jang SJ, Park JS, Shivakumar SB, Lee SL, Kang D, Byun JH, Park BW, Rho GJ. In vitro comparative analysis of human dental stem cells from a single donor and its neuronal differentiation potential evaluated by electrophysiology. Life Sci. 2016 Jun 1;154:39-51

25 Trainor PA, Krumlauf R. Patterning the cranial neural crest: hindbrain segmentation and Hox gene plasticity. Nat Rev Neurosci 2000;**1**:116-124.

26 Cobourne MT, Mitsiadis T. Neural crest cells and patterning of the mammalian dentition. J Exp Zool B Mol Dev Evol 2006;**306**:251-260.

27 Thompson H, Blentic A, Watson S, et al. The formation of the superior and jugular ganglia: insights into the generation of sensory neurons by the neural crest. Dev Dyn 2010;**239**:439-445.

28 About I, Bottero MJ, De Denato P, et al. Human dentin production in vitro. Exp Cell Res 2000;**258**:33-41.

29 Anand U, Otto WR, Facer P, et al. TRPA1 receptor localisation in the human peripheral nervous system and functional studies in cultured human and rat sensory neurons. Neurosci Lett 2008;**438**:221-227.

30 Bonnington JK, McNaughton PA. Signalling pathways involved in the sensitisation of mouse nociceptive neurones by nerve growth factor. J Physiol 2003;**551**:433-446.

31 Gervois P, Struys T, Hilkens P, Bronckaers A, Ratajczak J, Politis C, Brône B, Lambrichts I, Martens W. Neurogenic maturation of human dental pulp stem cells following neurosphere generation induces morphological and electrophysiological characteristics of functional neurons. Stem Cells Dev. 2015 Feb 1;24(3):296-311.

32 Kim JS, Kang JY, Ha JH, et al. Expression of nerve growth factor and matrix metallopeptidase-9/tissue inhibitor of metalloproteinase-1 in asthmatic patients. J Asthma 2013;**50**:712-717.

33 Chiaretti A, Pulitano S, Conti G, et al. Interleukin and neurotrophin up-regulation correlates with the severity of H1N1 infection in children: a case-controlled study. Int J Infect Dis 2013;**17**.

34 El-Hashim AZ, Jaffal SM. Nerve growth factor enhances cough and airway obstruction via TrkA receptor- and TRPV1-dependent mechanisms. Thorax 2009;**64**;791-797.

35 Belvisi MG, Birrell MA, Wortley MA, Maher SA, Satia I, Badri H, Holt K, Round P, McGarvey L, Ford J, Smith JA. XEN-D0501, a Novel TRPV1 Antagonist, Does Not Reduce Cough in Refractory Cough Patients. Am J Respir Crit Care Med. 2017 Jun 26. doi: 10.1164/rccm.201704-0769OC. [Epub ahead of print]

36 Wornle M, Sauter M, Kastenmuller K, et al. Novel role of toll-like receptor 3, RIG-I and MDA5 in poly (I:C) RNA-induced mesothelial inflammation. Mol Cell Biochem 2009;**322**:193-206.

37 Birring SS. The search for the hypersensitivity in chronic cough. Eur Respir J. 2017;49(2).

FIGURE LEGENDS

Figure 1: hDPSCs undergo both morphological and phenotype changes during neuronal differentiation to become functional PNEs. hDPSCs have a fibroblastic morphology consisting of splayed multipolar elongations (A). Following neuronal differentiation the cells lose this shape and take on a typical bipolar neuronal morphology consisting of a swollen cell body and axon-like projections (B). Undifferentiated hDPSCs express the fibroblast marker FSP (C). This FSP expression is lost during neuronal differentiation and is no longer expressed in PNEs (D). Prior to neuronal differentiation, hDPSCs do not express the specific neuronal markers PGP9.5 (E) or synaptophysin (G), which are present in PNE cultures (F and H respectively). PNEs exhibit voltage-activated Na^+ currents following 7 days differentiation. Family of inward currents recorded from a PNE following a series of 500 ms depolarising voltage steps from an initial holding potential -120 mV to 55 mV in 5 mV increments (I). This response, in the same cells, was completely inhibited in the presence of TTX (1 μM; J). I-V relationships in the absence and presence of TTX normalised against cell capacitance (K; n=7; mean cell capacitance: 38 pF, SEM: 2.85 (measured using pClamp software)). Bars represent SEM, ** $P < 0.01$, *** $P < 0.001$. TRPV1 expression in PNEs was shown by immunofluorescence (L). Whole cell patch clamping recording was carried out on PNEs to investigate the functional expression of TRPV1 channels. Addition of the TRPV1 agonist capsaicin during voltage ramp protocols increased both inward and outward membrane currents. This response was inhibited in the presence of the TRPV1 antagonist capsazepine (M). Peak currents were measured at -80 mV and 80 mV for statistical analysis (N).

Figure 2: The presence of TRPA1 channel proteins in PNEs was confirmed using immunofluorescence (A). Whole cell patch clamping recording was carried out on PNEs to

investigate the functional expression of TRPA1 channels. Addition of the TRPA1 agonist cinnamaldehyde during voltage ramp protocols increased both inward and outward membrane currents. This response was inhibited in the presence of the TRPA1 antagonist HC030031 (B). Peak currents were measured at -80 mV and 80 mV for statistical analysis (C). Application of cinnamaldehyde to isolated PNEs induced robust rises in $[Ca^{2+}]_i$ that were reversibly inhibited by subsequent application of HC030031 (D,E). In 9 cells the mean amplitude of cinnamaldehyde responses was significantly reduced from 1.96 $_{\Delta}F/F_0$ under control conditions to 0.02 $_{\Delta}F/F_0$ in the presence of HC030031, $p<0.01$, paired Student's t test (F). Error bars represent SEM. Cinnamaldehyde-induced elevations of $[Ca^{2+}]_i$ were concentration dependent and the mean EC_{50} value for this effect was 54 μM (95% confidence intervals 38-79 μM, n=4, Figs 2G&H, respectively).

Figure 3: PNE TRPA1 channels become hyper-responsive following 20 minutes incubation with the pro-inflammatory mediator NGF (100 ng/ml) but this effect was not apparent in PNEs incubated with NGF for 24hr they did not show heightened responses to cinnamaldehyde (100 μM; A). This hyper-responsiveness also appears to be independent of gene expression as no significant changes in TRPA1 gene expression in PNEs were observed following 6h and 24h NGF (100 ng/ml) treatments (B).

Figure 4: Poly I:C induces IL8 and IL6 secretion in PNE cultures. Supernatants taken from PNEs incubated with Poly I:C (2 μg/ml) for 24h showed increased IL8 and IL6 levels than those taken from untreated PNEs or PNEs incubated with Poly I:C for only 6h (A and B respectively). PNE TRPA1 channels become hyper-responsive following 20 minutes incubation with the viral mimetic Poly I:C (2 μg/ml). PNEs treated with Poly I:C

demonstrated heightened responses to the TRPA1 agonist cinnamaldehyde (100 μM) compared to those seen in untreated PNEs (C). This hyper-responsiveness appears to be independent of gene expression as no significant changes in TRPA1 gene expression in PNEs were observed following 6h and 24h Poly I:C treatments (D). Bars represent SEM, * $P < 0.05$, ** $P < 0.01$, *** $P<0.005$.

TRPA1 activation in a human sensory neuronal model: Relevance to cough hypersensitivity?

Rebecca Clarke PhD[a], Kevin Monaghan PhD[a], Imad About, PhD[b], Caoimhin S. Griffin, BSc[c], Gerard P. Sergeant, PhD[c], Ikhlas El Karim, PhD[a], J. Graham McGeown PhD[a], S. Louise Cosby PhD[a], Timothy M. Curtis PhD[a], Lorcan P. McGarvey MD[a]*, Fionnuala T. Lundy PhD[a*].

[a]Centre for Experimental Medicine, Wellcome-Wolfson Institute for Experimental Medicine, School of Medicine, Dentistry and Biomedical Sciences, Queen's University, Belfast, Northern Ireland

[b]Aix Marseille Université, CNRS, ISM UMR 7287, 13288, Marseille, France

[3]Smooth Muscle Research Centre, Dundalk Institute of Technology, Dundalk, Co. Louth, Ireland

*denotes joint senior authorship

Correspondence
Dr Lorcan McGarvey
Centre for Experimental Medicine
Wellcome-Wolfson Institute for Experimental Medicine
School of Medicine, Dentistry and Biomedical Sciences
97 Lisburn Road
Belfast
BT9 7BL
l.mcgarvey@qub.ac.uk

FUNDING

This work was funded by the National Centre for the Replacement, Refinement and Reduction of Animals in Research (NC3Rs) and the Pain Relief Foundation (UK).

ABSTRACT

The cough reflex becomes hyper-responsive in acute and chronic respiratory diseases, but understanding the underlying mechanism is hampered by difficulty accessing human tissue containing both nerve endings and neuronal cell bodies. We refined an adult stem-cell sensory neuronal model to overcome the limited availability of human neurones and applied the model to study transient receptor potential ankyrin 1 (TRPA1) channel expression and activation.

Human dental pulp stem cells (hDPSCs) were differentiated towards a neuronal phenotype, termed peripheral neuronal equivalents (PNEs). Using molecular and immunohistochemical techniques, together with Ca^{2+} microfluorimetry and whole cell patch clamping, we investigated roles for nerve growth factor (NGF) and the viral mimic Poly I:C in TRPA1 activation.

PNEs exhibited morphological, molecular and functional characteristics of sensory neurons and expressed functional TRPA1 channels. PNE treatment with NGF for 20 minutes generated significantly larger inward and outward currents compared to untreated PNEs in response to the TRPA1 agonist, cinnamaldehyde ($p<0.05$). PNE treatment with Poly I:C caused similar transient heightened responses to TRPA1 activation compared to untreated cells.

Using the PNE neuronal model we observed both NGF and Poly I:C mediated sensory neuronal hyper-responsiveness, representing potential neuro-inflammatory mechanisms associated with heightened nociceptive responses recognised in cough hypersensitivity syndrome.

Take home message

Development of a novel human adult stem cell neuronal model to investigate neural hyper-responsiveness in cough

INTRODUCTION

Airway sensory nerves control cough and represent a means by which the lung clears secretions and protects itself against inhaled foreign bodies and irritants[1]. In conditions such as asthma and chronic cough this neural reflex becomes hyper-responsive causing troublesome bouts of cough typically triggered by low level physical and chemical stimuli[2, 3]. These abnormal sensory responses often worsen during respiratory viral infections and while the effects of virus on airway epithelial and immune cells has been extensively studied little is known regarding the mechanisms responsible for airway neural hyper-responsiveness[4-6]. Although the symptoms associated with airway hyper-responsiveness are what disturb patients most about their condition, there are no current treatments that adequately alleviate and 'reset' this state[7]. Potential therapeutic targets include the transient receptor potential (TRP) cation channels which are responsible for sensing chemical and physical stimuli and are expressed on many cell types including airway sensory nerves[8]. We have previously shown that human rhinovirus upregulates expression of TRP ankyrin 1 (TRPA1) and TRP vanilloid 1 (TRPV1) channels in a neuronally differentiated immortalized human neuroblastoma cell line[9], however the mechanisms involved in nerve hyper-responsiveness remain to be investigated.

A number of neuroactive molecules are released into the airway following respiratory viral infection including nerve growth factor (NGF) which alters TRP channel function[10] and may be important in regulating airway sensory nerve responsiveness. In addition, sensory neurons are known to express Toll-like receptors (TLRs) which play a key role in host defence during microbial infection[11]. Toll-like receptor 3 (TLR 3) is of particular interest as it responds to viral double-stranded RNA (dsRNA), a by-product of replicating viruses including rhinovirus[12] and represents a potential route through which viral infection may induce cough reflex hyper-responsiveness.

Investigating TRP channel expression and regulation in human sensory neurons is challenging because the cell bodies of peripheral neurons are housed in neuronal ganglia which are not accessible by biopsy. Although TRP channel studies have been conducted in animal models[13-15] there are recognised interspecies differences in TRP function and expression[16-18]. Furthermore, in light of EU legislation for the protection of animals for scientific purposes there is an urgent need for development of a new generation of *in vitro* models based on human biology[19]. Thus, a human neuronal model could complement or potentially replace some animal models currently used in respiratory research and provide data that is relevant to human physiology.

Dental pulp tissue derives from migrating neural crest cells during development[20,21] and is a source of multipotential stem/progenitor cells. The propensity for human dental pulp stem cells (hDPSCs) to differentiate towards a neuronal phenotype, previously termed peripheral neuronal equivalents (PNEs), has been reported[22-24] and is likely to be explained by their neural crest origin. Neural crest stem cells are the main contributors to the development of peripheral nerve fibres, including those of the trigeminal ganglion of the trigeminal nerve[25, 26] and jugular ganglion of the vagus nerve[27]. Jugular ganglion C-fibres terminate within the extrapulmonary airways and respond directly to tussive stimuli such as capsaicin and bradykinin, express neuropeptides and tachykinins, and are thus considered important in nociceptive airway responses such as cough. Here we describe the development of a functional human *in vitro* neuronal model differentiated from hDPSCs, suitable for studying the role of neuroinflammatory factors in TRPA1 channel-mediated neuronal hyper-responsiveness.

Methods

Full details are available in the online supplement.

Cell culture and hDPSC enrichment

Human dental pulp cells were harvested from immature permanent third molar teeth in accordance with French ethics legislation[28] and maintained in minimal essential medium-alpha (MEM-alpha) supplemented with 10% fetal bovine serum (FBS), 100 UI/mL penicillin and 100 µg/mL streptomycin, L-glutamine and 200 µM ascorbic acid. hDPSCs were enriched in dental pulp cell cultures by preferential adhesion to fibronectin (10 µg/mL overnight at 4°C) coated 6-well plates and incubated at 37°C for 20 minutes. Non-adherent cells were discarded. hDPSCs were maintained on fibronectin for 2 days in MEM-alpha.

Neural Induction

hDPSCs were harvested from fibronectin-coated plates using trypsin and seeded onto plastic/glassware coated with poly-l-ornithine (0.01%) and laminin (5 µg/ml) and incubated with neurobasal A supplemented with B27, glutaMAX, human basic fibroblast growth factor (40 ng/mL) and epithelial growth factor (40 ng/ml) for 7 days.

Immunofluorescence

PNEs were differentiated from hDPSCs as described above on circular coverslips (16 mm, thickness 1). Cells were washed in phosphate buffered saline (PBS) and fixed by submerging in ice cold acetone for 8 minutes then air dried. Cells were washed in PBS and blocked for non-specific binding by incubation with 10% normal goat serum.

Cells were treated with specific primary antibody (Table S1; in 10% goat serum) overnight at 4°C. Appropriate anti-species Alexa Fluor secondary antibody conjugates were diluted in PBS containing 0.1% Triton X 100 and applied to cells for 1h at room temperature. Samples were mounted using ProLong Gold with DAPI and viewed using a fluorescent microscope.

qRT-PCR

Neural induction of hDPSCs towards PNEs was achieved as outlined above except that cells were grown in 96 well plates. Total RNA was harvested using the PicoPure RNA isolation kit and quantified using a Take3 plate and plate reader. RNA samples were reverse transcribed using the SuperScript VILO cDNA synthesis kit according to the manufacturer's instructions. qPCR reactions were set up using TaqMan universal mastermix with UNG according to the manufacturer's instructions using predesigned Taqman primers (Table S2, S3). qPCR was carried out using the Stratagene PCR instrument and analysed using Mx3005P software.

Whole Cell Patch Clamp

PNEs were differentiated as described on coverslips (thickness 0). Whole cell currents were recorded using borosilicate patch pipettes (2 – 5 MΩ resistance), an Axopatch 200B amplifier and pClamp9 software.

To measure voltage-gated Na+ channel activity, CsCl bath (150 mM NaCl, 6 mM CsCl, 1 mM MgCl2, 1.5 mM CaCl2, 5 mM glucose and 10 mM HEPES in dH2O. pH altered to 7.4 using Tris) and pipette (120 mM CsCl, 1 mM MgCl2, 4 mM Na2ATP, 10 mM BAPTA and 10 mM HEPES in dH2O. pH altered to 7.2 using Tris) solutions were used. 1 µM tetrodotoxin (TTX) was made up in CsCl bath solution. Experiments were carried out at room

temperature. The holding potential was -120 mV. Current-voltage (I-V) relationships were measured using a voltage step protocol.

TRP channel activity was recorded using a CsCl bath solution and a Cs-aspartate pipette solution (100 mM CsOH.2H2O, 100 mM aspartic acid, 20 mM CsCl, 1 mM MgCl2, 4 mM Na2ATP, 0.08 mM CaCl2, 10 mM BAPTA and 10 mM HEPES in dH2O. pH altered to 7.2 using Tris). 100 μM cinnamaldehyde, 10 μM HC030031, 10 μM capsaicin and 20 μM capsazepine were made up in CsCl bath solution. Experiments were carried out at 37°C. The holding potential was 0 mV throughout. I-V relationships were recorded using a voltage ramp protocol. All data were analysed using Clampfit9 software.

Microfluorimetric Calcium Imaging

For microfluorimetric calcium imaging PNEs were differentiated as described on coverslips (thickness 0). PNEs were loaded with Fura-2AM (5 μM) for 40 minutes at 37°C, placed into a recording chamber mounted on the stage of an inverted microscope and superfused with hanks (140 mM NaCl, 5 mM KCl, 2 mM CaCl2.2H2O, 1 mM MgCl2, 10 mM HEPES free acid and 5 mM glucose in dH2O. pH altered to 7.4 using NaOH). All solutions were kept at a 37°C using a water bath and perfusion system. [Ca2+]i was measured (details in online supplement) and TRP channel activity was observed as changes in [Ca2+]i following stimulation with 10 μM capsaicin and 10 μM capsazepine diluted in Hanks.

Confocal Ca2+ imaging

PNEs were loaded with 0.4μM fluo-4/AM for 6 minutes at room temperature and imaged using an iXon887 EMCCD camera (Andor Technology, Belfast) coupled to a Nipkow

spinning disk confocal head (CSU22, Yokogawa, Japan). A krypton-argon laser (Melles Griot UK) at 488 nm was used to excite the fluo-4, and the emitted light was detected at wavelengths >510 nm. Experiments were performed using a x60 objective (Olympus) and images were acquired at 15 frames per second. Background fluorescence from the camera, obtained using a null frame, was subtracted from each frame to obtain 'F'. F0 was determined as the minimum fluorescence under control conditions. The pseudo line-scan image and corresponding intensity profile plot (Figs 2D,E) were obtained using Image J software (NIH). ΔF/F0 refers to the measurement of the change in Ca2+ levels from basal to peak.

ELISA

PNEs were differentiated in 96 well plates. Supernatants were collected following treatments (as outlined below) and IL8 and IL6 levels were measured using human IL8 and IL6 DuoSet ELISA kits (R&D) according to the manufacturer's instructions.

Treatment of PNEs

PNEs were treated with pro-inflammatory cytokines (nerve growth factor (NGF; 100 ng/ml); interleukin 1β (IL1β; 5 ng/ml); tumour necrosis factor alpha (TNFα; 10 ng/ml)) and Poly I:C (2 μg/ml) for 20 minutes, 6h or 24h(Table S4). Control cells were incubated with medium alone.

Results

Enriched hDPSCs undergo neuronal differentiation to become functional PNEs

hDPSCs expressed the neural crest protein markers, P75, AP2α and HNK1 (Fig. S1) and displayed a fibroblastic morphology consisting of splayed multipolar elongations (Fig. 1A). Following 7 days neuronal differentiation, cells acquired a typical bipolar neuronal morphology with a centrally located swollen cell body and axon-like projections (Fig. 1B). Immunofluorescence confirmed a phenotype change from hDPSC to PNE during differentiation, manifest by loss of expression of the fibroblast marker FSP (Fig 1C, D) and gain of specific mature neuronal markers PGP9.5 (Fig. 1E, F) and synaptophysin (Fig. 1G, H). PNEs also expressed the neuropeptides substance P and CGRP, consistent with a sensory neuronal phenotype (Fig. S2).

Using whole cell patch clamping the neuronal phenotype of PNEs was further confirmed by demonstrating functional voltage-gated Na^+ (NaV) channels. Using Cs-based bath and pipette solutions to block outward K^+ currents, a family of rapidly inactivating inward currents were consistently generated when a series of 500 ms depolarising voltage steps were applied in 5 mV increments from an initial holding potential of -120 mV (Fig. 1I) to a final test potential of 55 mV. Currents were completely inhibited by the Na^+ channel inhibitor, TTX (1 μM) (Fig. 1J). Currents, normalised against cell capacitance, were plotted to show the I-V relationship (Fig. 1K).

Since TRPV1 has long been associated with a neuronal phenotype, its gene and protein expression in PNEs was determined by qPCR (Table S5) and immunofluorescene (Fig 1L). To confirm TRPV1 functionality in PNEs, whole cell patch clamping was performed using Cs^+-based bath and pipette solutions. Using a voltage ramp protocol, significant increases in both inward and outward currents were observed following application of the TRPV1 agonist

capsaicin (10 μM), which were significantly inhibited by capsazepine (20 μM; Fig. 1M, N). Vehicle only controls were unresponsive (Fig S3). To further confirm the suitability of PNEs for functional studies, microfluorimetric $[Ca^{2+}]_i$ imaging was performed for TRPV1 activity. Fura-loaded PNEs were shown to demonstrate spontaneous activity (Fig. S4), a characteristic of functional neurons, and upon capsaicin application an instantaneous increase in PNE $[Ca^{2+}]_i$ was observed (Fig. S5A), with $[Ca^{2+}]_i$ levels falling immediately afterwards. In the presence of the TRPV1 antagonist, capsazepine, PNE $[Ca^{2+}]_i$ did not increase above basal levels (Fig. S5B). The change in ratio with capsaicin in the absence and presence of capsazepine was graphed for statistical analysis (Fig. S5C).

PNEs express functional TRPA1

Having established the neuronal phenotype of PNEs (Fig. 1) their suitability for studying TRPA1 channels was investigated. TRPA1 gene expression was confirmed by qPCR (Table S5) along with protein expression by immunofluorescence (Fig. 2A). To study the functional TRPA1 on PNEs, whole cell patch clamp experiments were performed using Cs^+-based bath and pipette solutions. Using a voltage ramp protocol, significant increases in both inward and outward currents were observed in PNEs following application of cinnamaldehyde (100 μM) which were blocked by HC030031 (10 μM; Fig 2B,C). Vehicle only controls were unresponsive (Fig S3). To further confirm the suitability of PNEs for functional TRPA1 studies we examined the effect of cinnamaldehyde (100 μM) on Ca^{2+} levels in single PNEs using confocal Ca^{2+} imaging. Cinnamaldehyde induced robust rises in $[Ca^{2+}]_i$ that were reversibly inhibited by subsequent HC030031 application (see representative Figs. 2D,E and summary plot in Fig. 2F, n=9). Cinnamaldehyde responses were demonstrated to be concentration dependent (Figs 2G&H), with an EC_{50} of 54 μM. Using microfluorimetric

$[Ca^{2+}]_i$ imaging fura-loaded PNEs showed spontaneous activity (Fig. S4), and upon application of cinnamaldehyde an instantaneous increase in PNE $[Ca^{2+}]_i$ was observed (Fig. S6A), followed by falling $[Ca^{2+}]_i$ levels immediately afterwards. In the presenceHC030031, PNE $[Ca^{2+}]_i$ did not increase above basal levels (Fig. S6B). The mean change in ratio was graphed for statistical analysis (Fig. S6C).

NGF induces TRPA1 hyper-responsiveness on PNEs

NGF is known to induce hyper-responsiveness in sensory neurons [10, 29, 30] and is therefore a neuropathic cytokine worthy of investigating in this *in vitro* model. PNEs treated with NGF for 20 minutes immediately prior to patch clamp experiments generated significantly ($p < 0.05$) larger inward and outward currents when stimulated with cinnamaldehyde (Fig. 3A), demonstrating that PNE TRPA1 channels hyper-responsiveness in the presence of NGF. This hyper-responsive state was not sustained as PNEs treated for 24h did not generate the larger currents observed previously (Fig. 3A).

To investigate whether TRPA1 gene expression was altered following NGF treatment we undertook qRT-PCR on PNEs incubated with NGF for 6h and 24h. No significant changes in TRPA1 gene expression were observed (Fig. 3B). To determine whether this was an NGF-specific effect, we treated PNEs with the proinflammatory cytokines TNFα (10 ng/ml) and IL1β (5 ng/ml), and observed no significant change in TRPA1 gene expression (Fig. S7).

We also investigated whether similar effects in response to NGF treatment were observed in PNEs stimulated with capsaicin. No significant changes in capsaicin-induced currents were seen between untreated and NGF treated cells (Fig. S8A). Similarly, no changes were determined in TRPV1 gene expression following NGF treatment (Fig. S8B).

The viral mimetic Poly I:C induces IL8 release and TRPA1 hyper-responsiveness in PNEs

Poly I:C was employed to demonstrate the usefulness of the model to investigate the effects of viral infections on sensory neurons. Cell supernatants from PNEs incubated with Poly I:C were analysed for IL8 and IL6. Supernatants from control cells, and those incubated with Poly I:C for 6h showed no significant change in IL8 levels, and no detectable IL6 in controls (Fig. 4A, B). However, supernatants from cells incubated with Poly I:C for 24h had significantly higher levels of IL8 (2140.8 pg/ml) and IL6 (246.5 pg/ml) (Fig. 4A, B). Additional concentration and time-dependent effects of Poly I:C on IL8 levels are reported in Fig S9.

Poly I:C also induced TRPA1 hyper-responsiveness in PNEs. Treatment of PNEs with Poly I:C for 20 minutes immediately prior to patch clamping generated significantly larger inward and outward currents in response to cinnamaldehyde, compared with untreated PNEs (Fig. 4C). PNEs incubated with Poly I:C for 24h were not readily amenable to patch-clamp recording, suggesting changes had occurred in the plasma membrane. No significant changes were observed in TRPA1 gene expression following 6h or 24h Poly I:C treatments (Fig. 4D).

Discussion

In this study we successfully differentiated stem cells from human dental pulp towards PNEs which have morphological, molecular and functional characteristics of sensory neurons. We observed TRPA1 channel hyper-responsiveness following stimulation with both NGF and the viral mimic Poly I:C. Responses were rapid in onset, and independent of TRPA1 gene expression. Taken together our data suggest that PNEs represent a novel, species-specific *in vitro* model for the investigation of TRPA1 channel function and regulation on human

sensory neurons. We believe this model has potential to provide insight into the potential mechanisms involved in cough hypersensitivity.

An important refinement in our approach was the enrichment of hDPSCs from dental pulp cultures using differential fibronectin adhesion, allowing a phenotype switch from hDPSC to PNE in 7 days compared with 21 days previously reported using dental pulp cell cultures [22]. Functional neuronal activity in differentiated cells as described herein, should be considered a prerequisite for neuronal characterisation, particularly in view of the finding that voltage-dependent sodium channels are not present on hDPSCs[31].

To provide evidence for the suitability of PNEs as an *in vitro* model for the study of inflammatory TRP channel regulation we investigated the effect of the neurotrophic cytokine NGF. Levels of NGF are elevated in the airways of asthmatics[32] and in children with influenza infection airway NGF levels are increased and correlate with disease severity and cough duration[33] We observed that NGF rapidly induced increased TRPA1 activation consistent with that reported previously in primary cultures of mouse sensory neurons[28]. Such rapid effects are likely to be due to activation of intracellular cell signalling pathways resulting in phosphorylation of the TRP channel with subsequent channel hyper-responsiveness[9]. Our data suggest NGF can rapidly induce TRPA1 channel hyper-responsiveness, supporting a role for transcription-independent mechanisms in regulating TRP responses[10]. Interestingly, we did not see increased responses to capsaicin in NGF-treated cells, previously reported in a guinea pig model *in vivo*[34]. This disparity could serve to highlight differences between animal and human tissues and may add clinical relevance to the PNE model. It is also notable that positive preclinical data in animal models of the TRPV1 antagonist XEN-D0501 sharply contrasts the lack of efficacy reported in a placebo

controlled trial in chronic cough[35]. ~~This disparity could serve to highlight differences between animal and human tissues.~~

Following PNE treatment with the viral mimic Poly I:C significant increases in IL8 and IL6 secretion and increased currents in response to cinnamaldehyde, were observed compared to untreated PNEs. This is the first report to suggest a functional relationship between TRPA1 and Poly I:C. It is known that the viral mimetic Poly I:C mimics the pathogen associated molecular pattern (PAMP) dsRNA, and activates three pattern recognition receptors (PRRs) TLR3, retinoic acid-inducible gene 1 (RIG-I) and melanoma differentiation-associated protein 5 (MDA5)[~~35~~36]. Functional interactionsTRPA1 and Poly I:C could therefore be mediated *via* one or more of these receptors.

In conclusion, PNEs represent a novel species-specific *in vitro* model suitable for the study of TRP channel function and regulation on human sensory neurons which is in line with current EU and UK directives to replace, reduce and refine the use of animals in research[19]. Using this model we have demonstrated that NGF and the viral mimic Poly I:C directly and rapidly induce a TRP channel hyper-responsiveness on the cell membranes of human sensory nerves representing a possible neuro-inflammatory process responsible for cough reflex hyper-responsiveness. We have been careful to distinguish our experimental findings of neuronal hyper-responsiveness from neuronal hypersensitivity. Under experimental neuro-inflammatory conditions we observed an increased neural response for a given stimulus which may have a clinical parallel in the form of 'hypertussia' observed in patients with Cough Hypersensitivity Syndrome (CHS) [37]. We have yet to determine if our PNE model can be rendered 'hypersensitive' to low level stimulation. CHS is a disorder gaining increasing recognition amongst respiratory, allergy, gastroenterology, speech/voice and otolaryngology healthcare professionals[38]. There is a need to improve our understanding of the neurobiology of this condition and we believe the novel techniques we report in this

Formatted: Left

manuscript and the clinical relevance of our experimental findings will be of interest to those working in this field.

Acknowledgements

We acknowledge the skilful technical assistance of Catherine Fulton.

REFERENCES

1 Canning BJ, Chang AB, Bolser DC, et al. Anatomy and neurophysiology of cough: CHEST Guideline and Expert Panel report. Chest 2014;**146**:1633-1648.

2 Chung KF, McGarvey L, Mazzone SB. Chronic cough as a neuropathic disorder. Lancet Respir Med. 2013;**1**(5):414-22.

3 Morice AH, Millqvist E, Belvisi MG, et al. Expert opinion on the cough hypersensitivity syndrome in respiratory medicine. Eur Respir J. 2014;44(5):1132-48

4 McErlean P, Favoreto S Jr, Costa FF, et al. Human rhinovirus infection causes different DNA methylation changes in nasal epithelial cells from healthy and asthmatic subjects. BMC Med Genomics 2014;**7**.

5 Patel DA, You Y, Huang G, et al. Interferon response and respiratory virus control are preserved in bronchial epithelial cells in asthma. J Allergy Clin Immunol 2014;**134**:1402-1412.

6 Guo H, Baker SF, Martinez-Sobrido L, et al. Induction of CD8 T cell heterologous protection by a single dose of single-cycle infectious influenza virus. J Virol 2014;**88**:12006-12016.

7 McGarvey L, McKeagney P, Polley L, et al. Are there clinical features of a sensitized cough reflex? Pulm Pharmacol Ther 2009;**22**:59-64.

8 Bessac BF, Jordt SE. Breathtaking TRP channels: TRPA1 and TRPV1 in airway chemosensation and reflex control. Physiology 2008;**23**:360-370.

9 Abdullah H, Heaney LG, Cosby SL, et al. Rhinovirus upregulates transient receptor potential channels in a human neuronal cell line: implications for respiratory virus-induced cough reflex sensitivity. Thorax 2014;**69**:46-54.

10 Ji RR, Samad TA, Jin SX, et al. p38 MAPK activation by NGF in primary sensory neurons after inflammation increases TRPV1 levels and maintains heat hyperalgesia. Neuron 2002;**36**:57-68.

11 Lafon M, Megret F, Lafage M, et al. The innate immune facet of brain: human neurons express TLR3 and sense viral dsRNA. J Mol Neurosci 2006;**29**:184-194.

12 Jacobs BL, Langland JO. When two strands are better than one: the mediators and modulators of the cellular responses to double-stranded RNA. Virology 1996;**219**:339-349.

13 Honore P, Chandran P, Hernandez G, et al. Repeated dosing of ABT-102, a potent and selective TRPV1 antagonist, enhances TRPV1-mediated analgesic activity in rodents, but attenuates antagonist-induced hyperthermia. Pain 2009;**142**:27-35.

14 Malek S, Sample SJ, Schwartz Z, et al. Effect of analgesic therapy on clinical outcome measures in a randomized controlled trial using client-owned dogs with hip osteoarthritis. BMC Vet Res 2012;**8**.

15 de la Roche J, Eberhardt MJ, Klinger AB, et al. The molecular basis for species-species activation of human TRPA1 protein by protons involves poorly conserved residues within transmembrane domains 5 and 6. J Biol Chem 2013;**288**:20280-20292.

16 Jordt SE, Julius D. Molecular basis for species-specific sensitivity to "hot" chilli peppers. Cell 2002;**108**:421-430.

17 Klionsky L, Tamir R, Gao B, et al. Species-specific pharmacology of Trichloro(sulfanyl)ethyl benzamides as transient receptor potential ankyrin 1 (TRPA1) antagonists. Mol Pain 2007;**3**.

18 Bianchi BR, Zhang XF, Reilly RM, et al. Species comparison and pharmacological characterization of human, monkey, rat, and mouse TRPA1 channels. J Phatmacol Exp Ther 2012;**341**:360-368.

19 European Commission Directive 2010/63/EU. Legislation for the protection of animals used for scientific purposes.

20 d'Aquino R, De Rosa A, Laino G, et al. Human dental pulp stem cells: from biology to clinical applications. J Exp Zool B Mol Dev Evol 2009;**312B**:408-415.

21 Coura GS, Garcez RC, de Aquiar CB, et al. Human periodontal ligament: a niche of neural crest stem cells. J Periodontal Res 2008;**43**:531-536.

22 Arthur A, Rychkov G, Shi S, et al. Adult human dental pulp stem cells differentiate toward functionally active neurons under appropriate environmental cues. Stem Cells 2008;**26**:1787-1795.

23 Urraca N, Memon R, El-Iyachi I, et al. Characterization of neurons from immortalized dental pulp stem cells for the study of neurogenetic disorders. Stem Cell Res. 2015 Nov;15(3):722-30.

24 Ullah I, Subbarao RB, Kim EJ, Bharti D, Jang SJ, Park JS, Shivakumar SB, Lee SL, Kang D, Byun JH, Park BW, Rho GJ. In vitro comparative analysis of human dental stem cells from a single donor and its neuronal differentiation potential evaluated by electrophysiology. Life Sci. 2016 Jun 1;154:39-51

25 Trainor PA, Krumlauf R. Patterning the cranial neural crest: hindbrain segmentation and Hox gene plasticity. Nat Rev Neurosci 2000;**1**:116-124.

26 Cobourne MT, Mitsiadis T. Neural crest cells and patterning of the mammalian dentition. J Exp Zool B Mol Dev Evol 2006;**306**:251-260.

27 Thompson H, Blentic A, Watson S, et al. The formation of the superior and jugular ganglia: insights into the generation of sensory neurons by the neural crest. Dev Dyn 2010;**239**:439-445.

28 About I, Bottero MJ, De Denato P, et al. Human dentin production in vitro. Exp Cell Res 2000;**258**:33-41.

29 Anand U, Otto WR, Facer P, et al. TRPA1 receptor localisation in the human peripheral nervous system and functional studies in cultured human and rat sensory neurons. Neurosci Lett 2008;**438**:221-227.

30 Bonnington JK, McNaughton PA. Signalling pathways involved in the sensitisation of mouse nociceptive neurones by nerve growth factor. J Physiol 2003;**551**:433-446.

31 Gervois P, Struys T, Hilkens P, Bronckaers A, Ratajczak J, Politis C, Brône B, Lambrichts I, Martens W. Neurogenic maturation of human dental pulp stem cells following neurosphere generation induces morphological and electrophysiological characteristics of functional neurons. Stem Cells Dev. 2015 Feb 1;24(3):296-311.

32 Kim JS, Kang JY, Ha JH, et al. Expression of nerve growth factor and matrix metallopeptidase-9/tissue inhibitor of metalloproteinase-1 in asthmatic patients. J Asthma 2013;**50**:712-717.

33 Chiaretti A, Pulitano S, Conti G, et al. Interleukin and neurotrophin up-regulation correlates with the severity of H1N1 infection in children: a case-controlled study. Int J Infect Dis 2013;**17**.

34 El-Hashim AZ, Jaffal SM. Nerve growth factor enhances cough and airway obstruction via TrkA receptor- and TRPV1-dependent mechanisms. Thorax 2009;**64**;791-797.

~~34~~35 Belvisi MG, Birrell MA, Wortley MA, Maher SA, Satia I, Badri H, Holt K, Round P, McGarvey L, Ford J, Smith JA. XEN-D0501, a Novel TRPV1 Antagonist, Does Not Reduce Cough in Refractory Cough Patients. Am J Respir Crit Care Med. 2017 Jun 26. doi: 10.1164/rccm.201704-0769OC. [Epub ahead of print]

36 Wornle M, Sauter M, Kastenmuller K, et al. Novel role of toll-like receptor 3, RIG-I and MDA5 in poly (I:C) RNA-induced mesothelial inflammation. Mol Cell Biochem 2009;**322**:193-206.

~~35~~37 Birring SS. The search for the hypersensitivity in chronic cough. Eur Respir J. 2017;49(2).

FIGURE LEGENDS

Figure 1: hDPSCs undergo both morphological and phenotype changes during neuronal differentiation to become functional PNEs. hDPSCs have a fibroblastic morphology consisting of splayed multipolar elongations (A). Following neuronal differentiation the cells lose this shape and take on a typical bipolar neuronal morphology consisting of a swollen cell body and axon-like projections (B). Undifferentiated hDPSCs express the fibroblast marker FSP (C). This FSP expression is lost during neuronal differentiation and is no longer expressed in PNEs (D). Prior to neuronal differentiation, hDPSCs do not express the specific neuronal markers PGP9.5 (E) or synaptophysin (G), which are present in PNE cultures (F and H respectively). PNEs exhibit voltage-activated Na^+ currents following 7 days differentiation. Family of inward currents recorded from a PNE following a series of 500 ms depolarising voltage steps from an initial holding potential -120 mV to 55 mV in 5 mV increments (I). This response, in the same cells, was completely inhibited in the presence of TTX (1 μM; J). I-V relationships in the absence and presence of TTX normalised against cell capacitance (K; n=7; mean cell capacitance: 38 pF, SEM: 2.85 (measured using pClamp software)). Bars represent SEM, ** $P < 0.01$, *** $P < 0.001$. TRPV1 expression in PNEs was shown by immunofluorescence (L). Whole cell patch clamping recording was carried out on PNEs to investigate the functional expression of TRPV1 channels. Addition of the TRPV1 agonist capsaicin during voltage ramp protocols increased both inward and outward membrane currents. This response was inhibited in the presence of the TRPV1 antagonist capsazepine (M). Peak currents were measured at -80 mV and 80 mV for statistical analysis (N).

Figure 2: The presence of TRPA1 channel proteins in PNEs was confirmed using immunofluorescence (A). Whole cell patch clamping recording was carried out on PNEs to

investigate the functional expression of TRPA1 channels. Addition of the TRPA1 agonist cinnamaldehyde during voltage ramp protocols increased both inward and outward membrane currents. This response was inhibited in the presence of the TRPA1 antagonist HC030031 (B). Peak currents were measured at -80 mV and 80 mV for statistical analysis (C). Application of cinnamaldehyde to isolated PNEs induced robust rises in $[Ca^{2+}]_i$ that were reversibly inhibited by subsequent application of HC030031 (D,E). In 9 cells the mean amplitude of cinnamaldehyde responses was significantly reduced from 1.96 $_{\Delta}F/F_0$ under control conditions to 0.02 $_{\Delta}F/F_0$ in the presence of HC030031, $p<0.01$, paired Student's t test (F). Error bars represent SEM. Cinnamaldehyde-induced elevations of $[Ca^{2+}]_i$ were concentration dependent and the mean EC_{50} value for this effect was 54 μM (95% confidence intervals 38-79 μM, n=4, Figs 2G&H, respectively).

Figure 3: PNE TRPA1 channels become hyper-responsive following 20 minutes incubation with the pro-inflammatory mediator NGF (100 ng/ml) but this effect was not apparent in PNEs incubated with NGF for 24hr they did not show heightened responses to cinnamaldehyde (100 μM; A). This hyper-responsiveness also appears to be independent of gene expression as no significant changes in TRPA1 gene expression in PNEs were observed following 6h and 24h NGF (100 ng/ml) treatments (B).

Figure 4: Poly I:C induces IL8 and IL6 secretion in PNE cultures. Supernatants taken from PNEs incubated with Poly I:C (2 μg/ml) for 24h showed increased IL8 and IL6 levels than those taken from untreated PNEs or PNEs incubated with Poly I:C for only 6h (A and B respectively). PNE TRPA1 channels become hyper-responsive following 20 minutes incubation with the viral mimetic Poly I:C (2 μg/ml). PNEs treated with Poly I:C

demonstrated heightened responses to the TRPA1 agonist cinnamaldehyde (100 μM) compared to those seen in untreated PNEs (C). This hyper-responsiveness appears to be independent of gene expression as no significant changes in TRPA1 gene expression in PNEs were observed following 6h and 24h Poly I:C treatments (D). Bars represent SEM, * $P < 0.05$, ** $P < 0.01$, *** $P<0.005$.

Figure 1

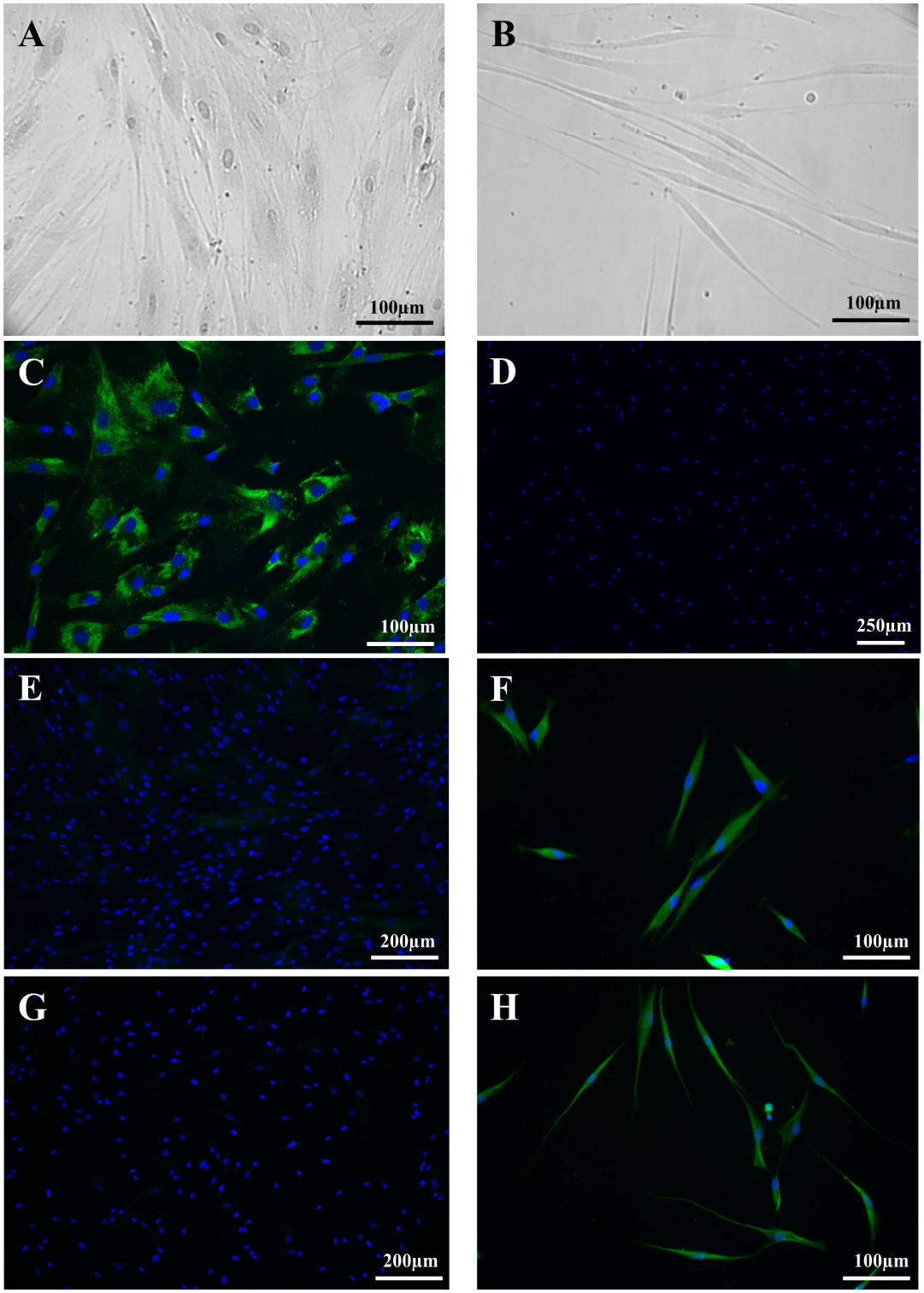

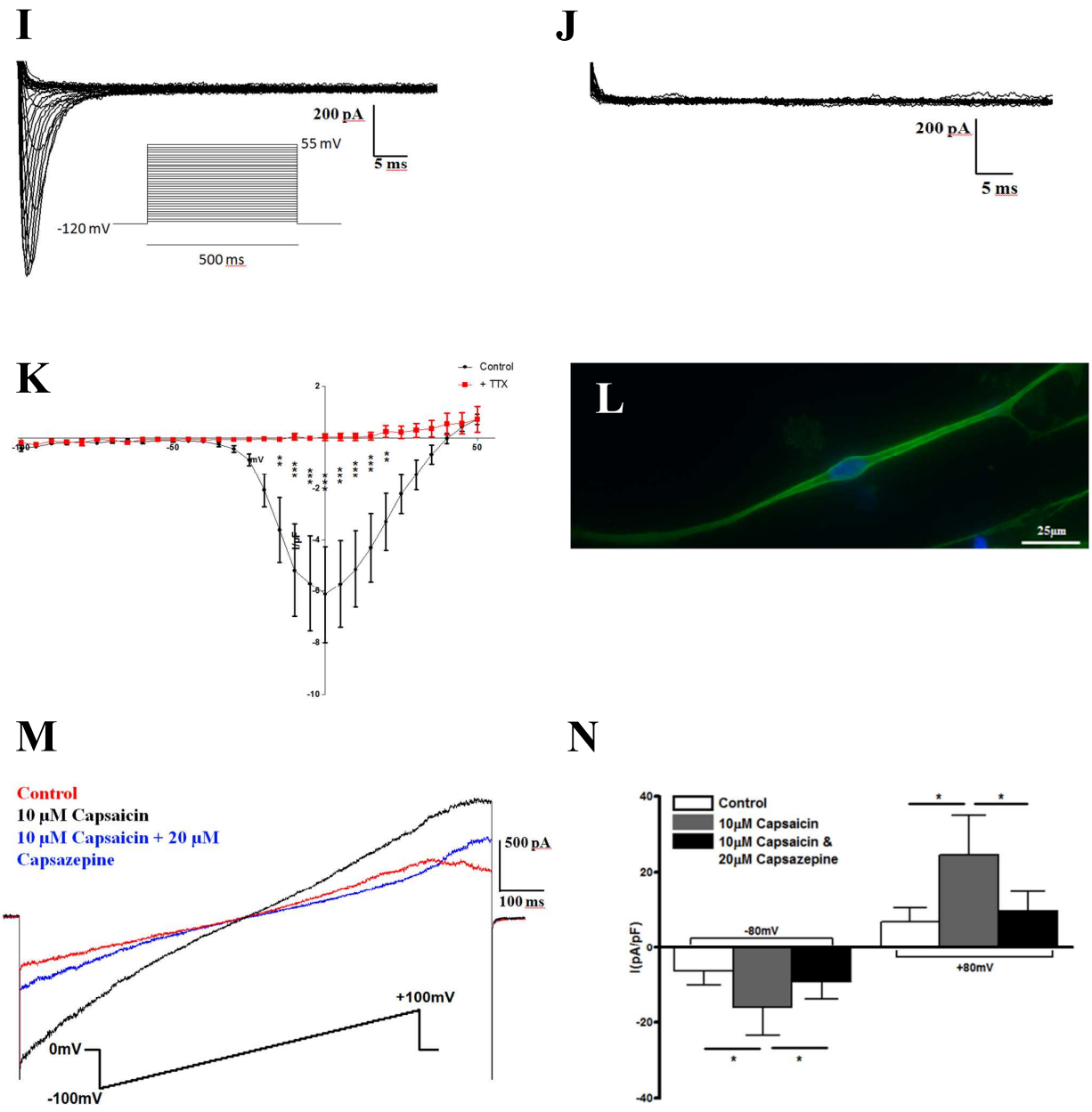
I
200 pA
55 mV
5 ms
-120 mV
500 ms
J
200 pA
5 ms
K
Control
+ TTX
L
25μm
M
Control
10 μM Capsaicin
10 μM Capsaicin + 20 μM Capsazepine
500 pA
100 ms
+100mV
0mV
-100mV
N
Control
10μM Capsaicin
10μM Capsaicin & 20μM Capsazepine
I(pA/pF)
-80mV
+80mV

Figure 2

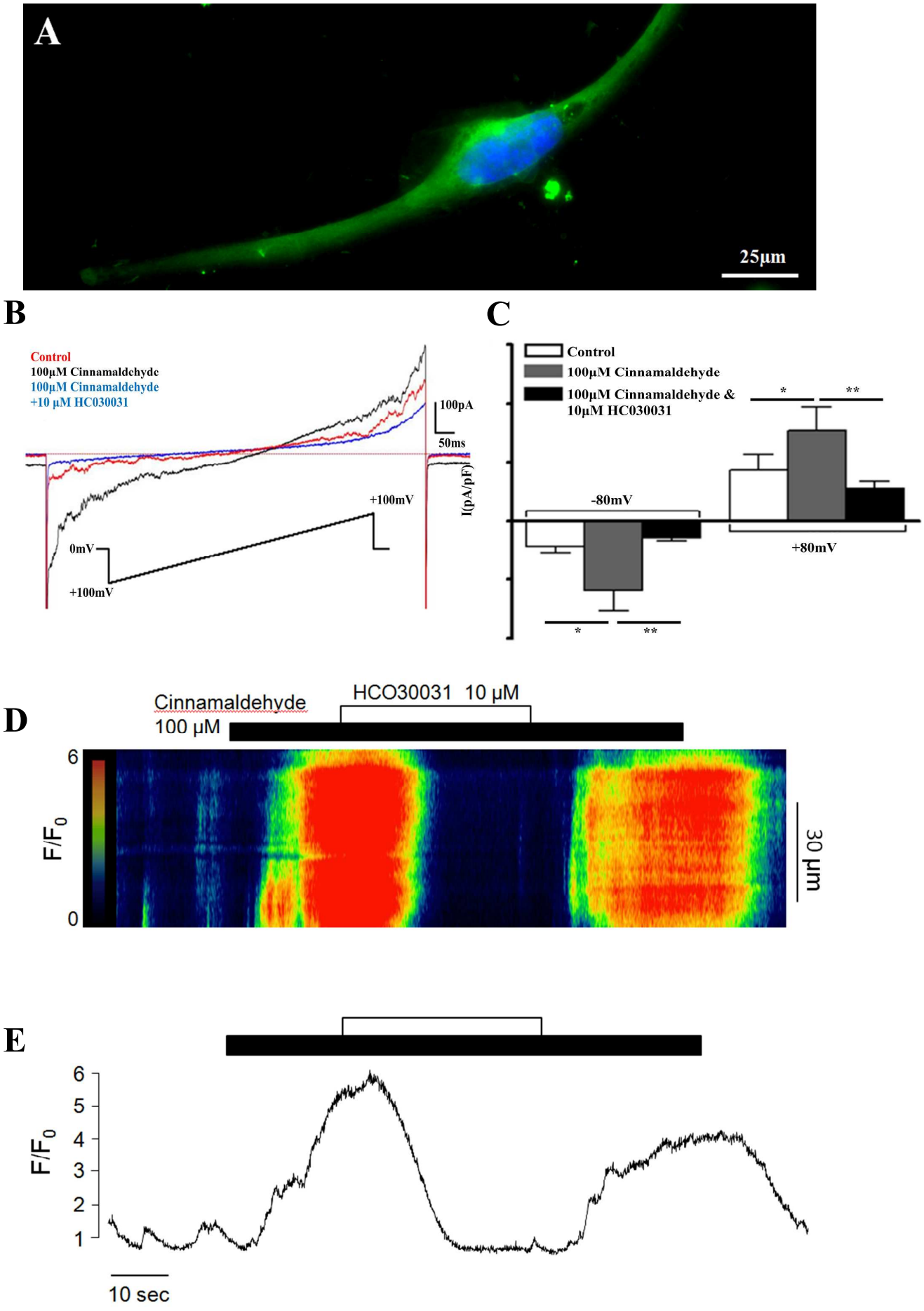
A
25μm
B
Control
100μM Cinnamaldehyde
100μM Cinnamaldehyde
+10 μM HC030031
100pA
50ms
I(pA/pF)
+100mV
0mV
+100mV
C
Control
100μM Cinnamaldehyde
100μM Cinnamaldehyde &
10μM HC030031
*
**
-80mV
+80mV
*
**
D
Cinnamaldehyde
100 μM
HCO30031 10 μM
6
F/F0
0
30 μm
E
6
5
4
3
2
1
F/F0
10 sec

F

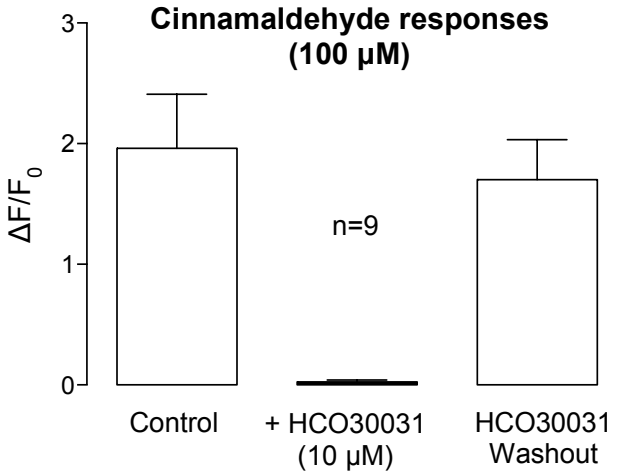
Cinnamaldehyde responses
(100 µM)
ΔF/F0
3
2
1
0
n=9
Control
+ HCO30031
(10 µM)
HCO30031
Washout

G

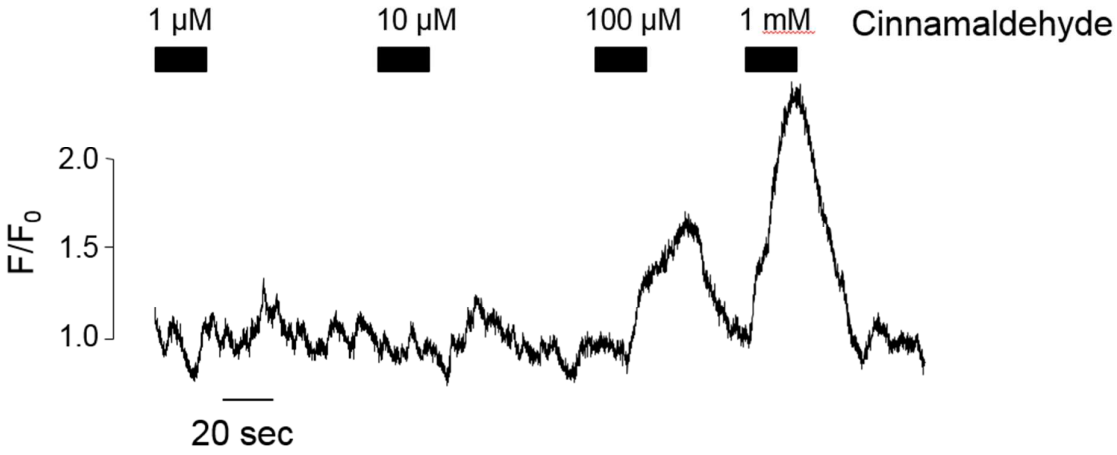
1 µM
10 µM
100 µM
1 mM
Cinnamaldehyde
F/F0
2.0
1.5
1.0
20 sec

H

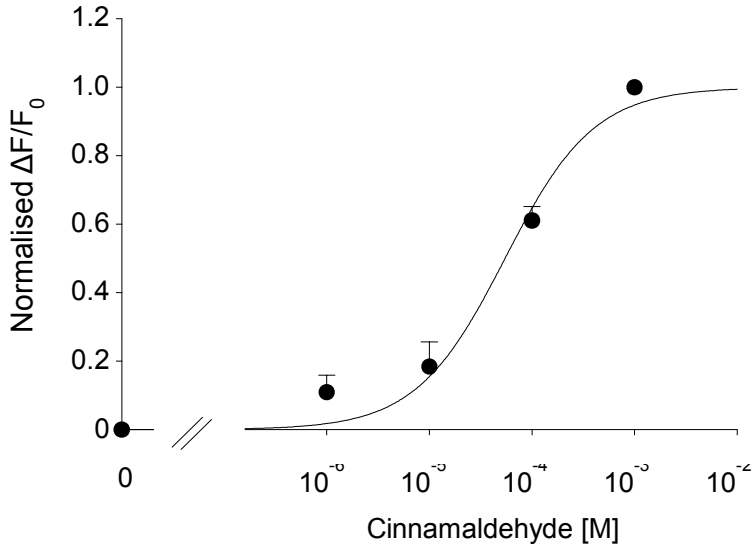
Normalised ΔF/F0
1.2
1.0
0.8
0.6
0.4
0.2
0
0
Cinnamaldehyde [M]

Figure 3

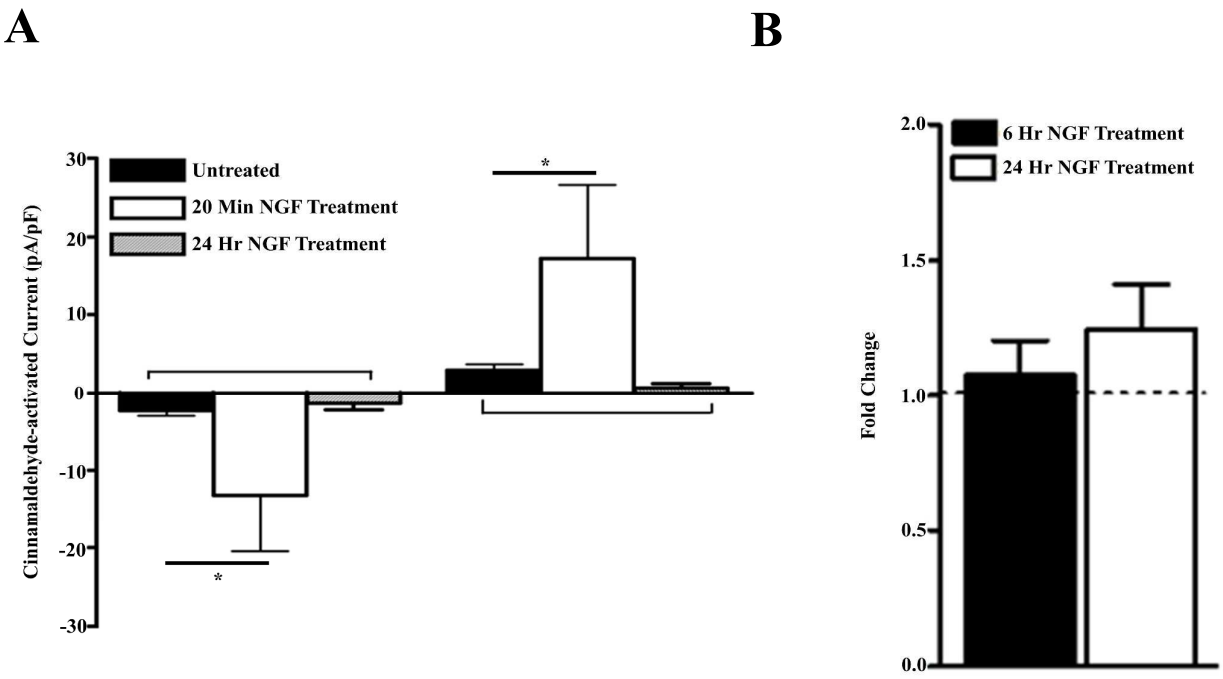
A
B
Untreated
20 Min NGF Treatment
24 Hr NGF Treatment
Cinnamaldehyde-activated Current (pA/pF)
30
20
10
0
-10
-20
-30
*
*
6 Hr NGF Treatment
24 Hr NGF Treatment
Fold Change
2.0
1.5
1.0
0.5
0.0

Figure 4

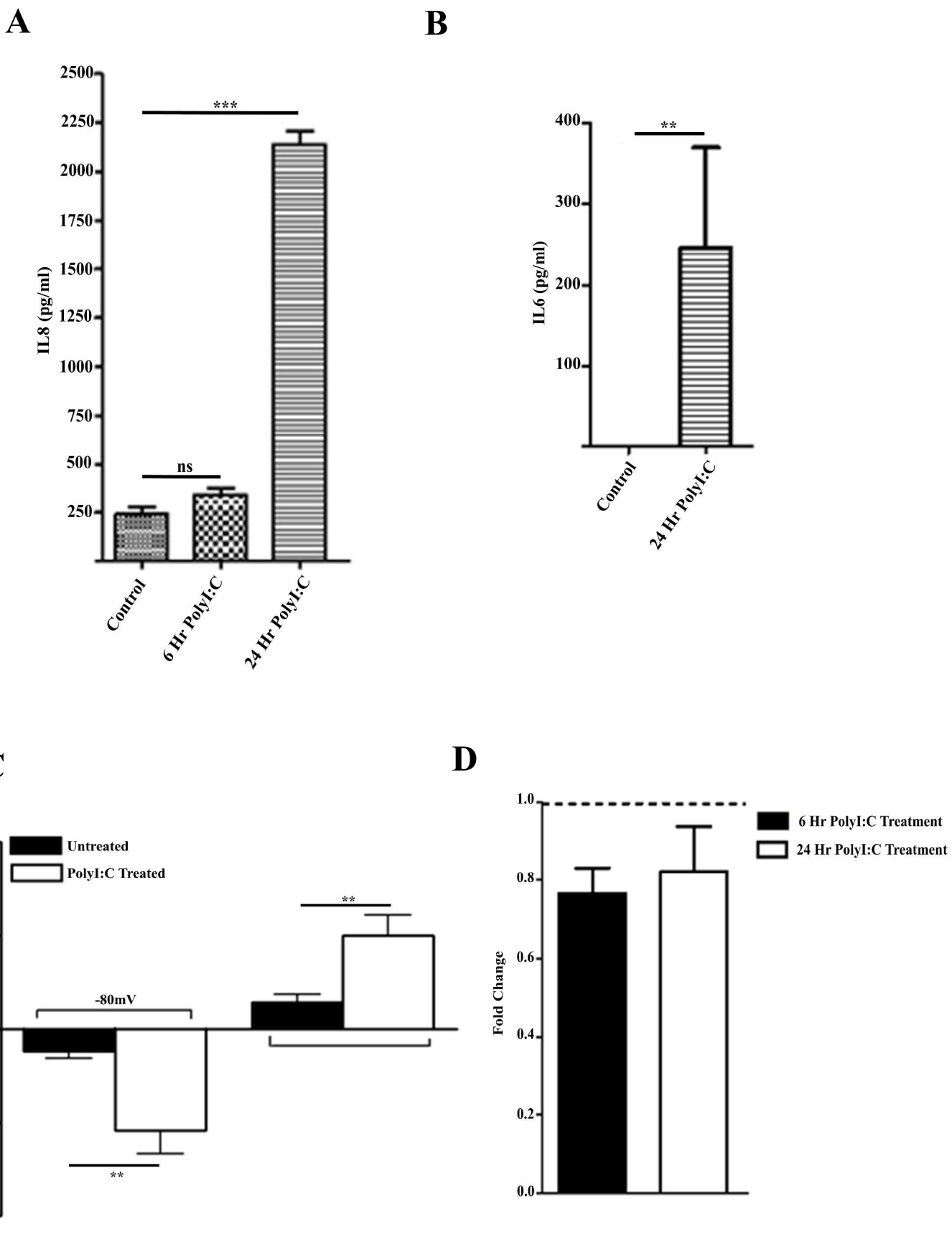
A
IL8 (pg/ml)
2500
2250
2000
1750
1500
1250
1000
750
500
250
***
ns
Control
6 Hr PolyI:C
24 Hr PolyI:C
B
IL6 (pg/ml)
400
300
200
100
**
Control
24 Hr PolyI:C
C
Untreated
PolyI:C Treated
Cinnamaldehyde-activated Current (pA/pF)
20
10
0
-10
-20
-80mV
**
**
D
Fold Change
1.0
0.8
0.6
0.4
0.2
0.0
6 Hr PolyI:C Treatment
24 Hr PolyI:C Treatment

ONLINE SUPPLEMENT

MATERIALS AND METHODS

Table S1: List of primary antibodies, their source and working dilutions

Antibody	Source	Host Species	Working Concentration
FSP	Abcam (UK)	Mouse	1:500
P75	Advanced Targetting Systems (USA)	Mouse	1:100
HNK1	Sigma (UK)	Mouse	1:100
AP2α	Novus Biologicals (USA)	Rabbit	1:50
PGP9.5	Cedarlane (Canada)	Mouse	1:250
Synaptophysin	Dako (UK)	Rabbit	1:50 (Pre-diluted)
SP	In house (Eedy et al., 91)	Rabbit	1:1000
CGRP	Peninsula (USA)	Rabbit	1:900
TRPA1	Abcam (UK)	Rabbit	1:100
TRPV1	Abnova (Taiwan)	Mouse	1:100

Harvesting total RNA

RNA was extracted from each sample (1 well) using the Picopure RNA Isolation kit as follows: culture medium was removed from PNE cultures and cells were washed with ice cold PBS for 5 minutes. Extraction buffer (100 µl) was then added and samples were incubated at 42°C for 30 minutes. Each sample was mixed gently using a pipette tip and collected in a microcentrifuge tube.

RNA purification columns were preconditioned by adding conditioning buffer (250 µl) to each column membrane. Membranes were incubated with the conditioning buffer for 5 minutes at room temperature. Columns were then centrifuged at high speed for 1 minute to remove buffer.

70% ethanol (100 µl) was added to each microcentrifuge containing the cell extract and samples were mixed gently by pipetting. The mixture was transferred to a preconditioned RNA purification column and RNA was bound to the column by centrifuging the column at low speed for 2 minutes. Flowthrough was removed by centrifuging the column at high speed for 30 seconds. Wash buffer 1 (100 µl) was added to each column and centrifuged for 1 minute at 8,000 x g. Wash buffer 2 (100 µl) was then added to each column and samples were centrifuged for 1 minute at 8,000 x g. A second aliquot of wash buffer 2 (100 µl) was added to each column and centrifuged at high speed for 2 minutes. The purification column was then transferred to a collection tube and elution buffer (11 µl) was applied directly to the column membrane. Membranes were incubated with elution buffer for 1 minute at room temperature before being centrifuged for 1 minute at 1000 x g to ensure complete coverage of the membrane with the buffer. RNA was then eluted by centrifuging for 1 minute at high speed.

RNA was quantified using 2 µl of cDNA solution on a Take3 plate. Absorbance readings at 260 nm and 280 nm were obtained along with a 260/280 ratio and the concentration of RNA per µl.

S2: TaqMan primer details

Gene	Reference No.	Chromosome No.	Probe sits on exon boundary	Base position	Amplicon length
TRPA1	HS00175798	8	2 - 3	441	124
TRPV1	HS00218912	17	8 - 9	1540	94
B2M	HS00984230	15	3 - 4	431	81
GUSB	HS00939627	7	8 - 9	1522	96

Table S3: Thermal profile for qPCR

Segment	Thermal profile	Cycles
1	2 minutes at 55°C	1
2	10 minutes at 95°C	1
3	15 seconds at 95°C 1 minute at 60°C	45

Microfluorimetric Calcium Imaging

$[Ca^{2+}]_i$ was measured by alternating excitation wavelengths of 340 and 380 nm light delivered from a dual monochromator (5 nm bandwidth) using a light chopper. Emitted fluorescence was measured from the side port of the microscope via an adjustable rectangular window, a filter (510 nm) and a photomultiplier tube (PMT) in the light path. Fluorescence equipment was controlled by Acquisition Engine software. Background fluorescence was measured at the end of each experiment by exposing the cell to 5 mM MnCl2 and quenching the fluorescent dye. Changes in the background-corrected fluorescence emitted at each excitation wavelength (R=340/380) was used as a measure of change in cytoplasmic Ca^{2+} concentrations.

Table S4: Cytokine details

Cytokine	Source
NGF	Peprotech (USA)
TNFα	Sigma (UK)
IL1β	Sigma (UK)
Poly I:C	Invivogen (UK)

RESULTS

Table S5: The presence of TRPA1 and TRPV1 mRNA in PNEs was confirmed by qPCR

Channel	Ct	Average Ct
TRPA1	25.785	25.547
	25.865	
	26.055	
	24.755	
	25.275	
TRPV1	34.94	34.644
	34.415	
	35.155	
	33.935	
	34.775	

FIGURE LEGENDS

Figure S1: hDPSCs express the neural crest stem cell marker P75 (A) and subpopulations of cells express HNK1 (B) and AP2α (C). Scale bars: 50 μm.

Figure S2: PNEs express the neuropeptides SP (A) and CGRP (B), a characteristic of sensory neurons. Scale bar 100 μm.

Figure S3: PNEs displayed spontaneous fluctuations in $[Ca^{2+}]_i$. Viability of PNEs was determined through the observation of increases in $[Ca^{2+}]_i$ in the absence of agonist challenges. Figures A and B are representative traces of the varying degrees of spontaneous activity observed in PNEs.

Figure S4: Changes in intracellular Ca^{2+} levels ($[Ca^{2+}]_i$) in response to capsaicin were investigated in PNEs demonstrating spontaneous activity. Stimulation with capsaicin evoked an instantaneous increase in $[Ca^{2+}]_i$ levels (A). $[Ca^{2+}]_i$ fell back to basal levels immediately after peaking. In the presence of the TRPV1 antagonist capsazepine PNEs exhibited an attenuated response to capsaicin compared with cells that had not been exposed to the antagonist (B). The change in absorbance ratio (ΔRatio) was graphed for statistical analysis to show specific TRPV1 activation in PNEs (C). Bars represent SEM, * $P < 0.05$, ** $P < 0.01$.

Figure S5: PNEs demonstrating spontaneous activity were stimulated with cinnamaldehyde and an instantaneous increase in $[Ca^{2+}]_i$ levels was observed (A). $[Ca^{2+}]_i$ fell back to basal levels immediately after peaking. In the presence of the TRPA1 antagonist HC030031 PNEs exhibited an attenuated response to cinnamaldehyde compared to cells that had not been exposed to the antagonist (B). The change in absorbance ratio (ΔRatio) was graphed for statistical analysis to show specific TRPA1 activation in PNEs (C). Bars represent SEM, * $P < 0.05$, ** $P < 0.01$.

Figure S6: PNEs were treated with pro-inflammatory cytokines TNFα and IL1β to determine whether the lack of change in TRPA1 gene expression was specific to NGF treated cells. No significant changes in TRPA1 gene expression was observed in PNEs treated with either TNFα or IL1β. Bars represent SEM.

Figure S7: PNE TRPV1 channels did not become hyper-responsive following 20 minutes incubation with the pro-inflammatory mediator NGF (100 ng/ml) (A). Similarly there were no significant changes in TRPV1 gene expression following NGF treatment for 6 or 24 hours (B). Bars represent SEM, * $P < 0.05$.

Figure S8: Vehicle controls. PNE currents were not altered in response to 0.001% DMSO alone. Currents generated by cinnamaldehyde and capsaicin were included for comparison. Bars represent SEM.

Figure S9: PNEs were treated with a range of Poly I:C concentrations (2 μg/ml – 20 μg/ml) in order to determine the optimal working concentration for experiments. IL8 release was used a measure of response. PNEs treated with 2 μg/ml PolyI:C generated the largest response in terms of IL8 release compared to 10 μg/ml and 20 μg/ml and thus was selected for use in further experiments. Bars represent SEM, *** $P < 0.001$.

FIGURES

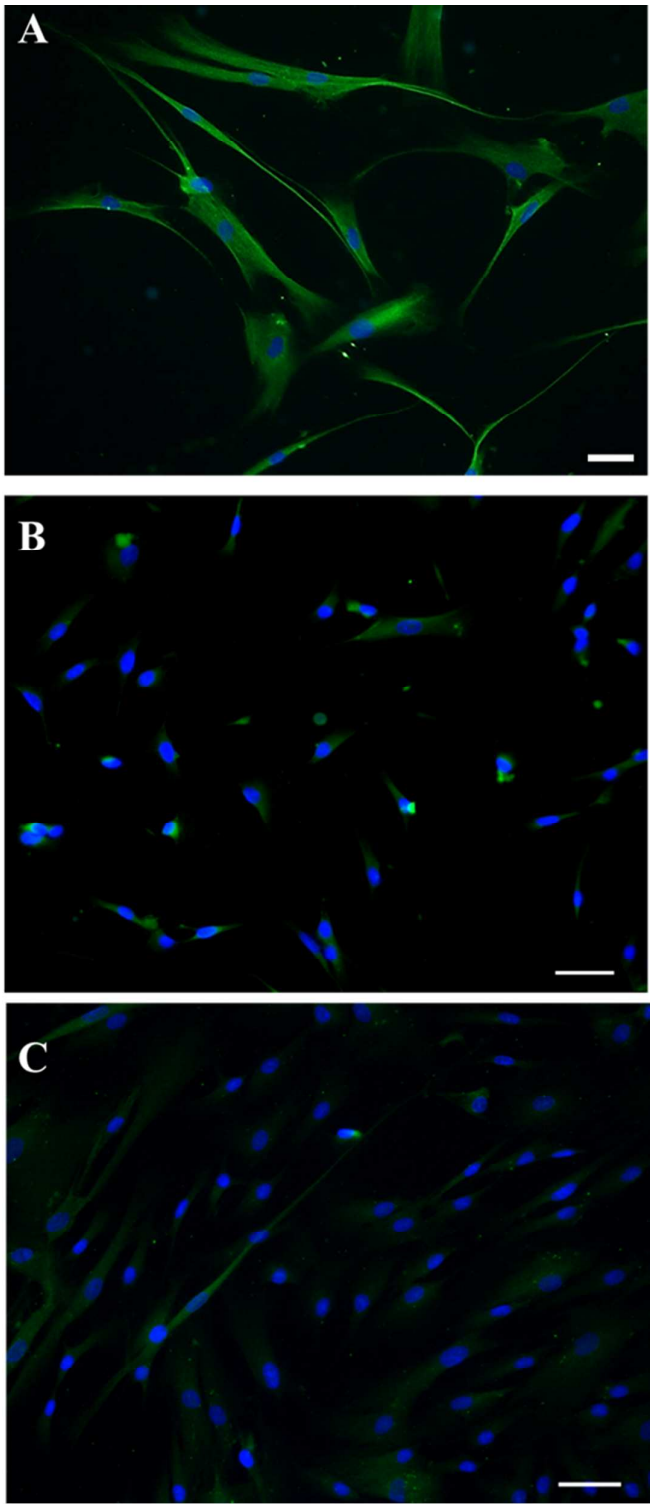

Figure S1

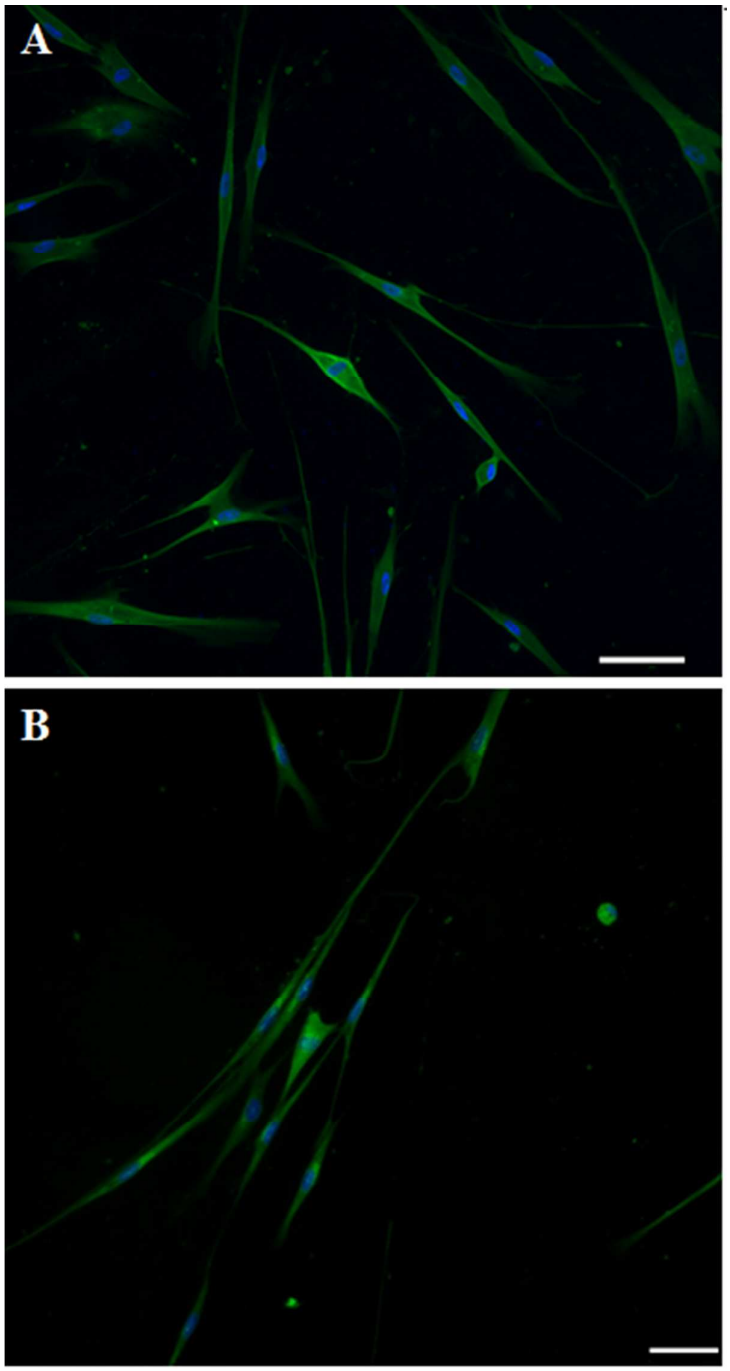

Figure S2

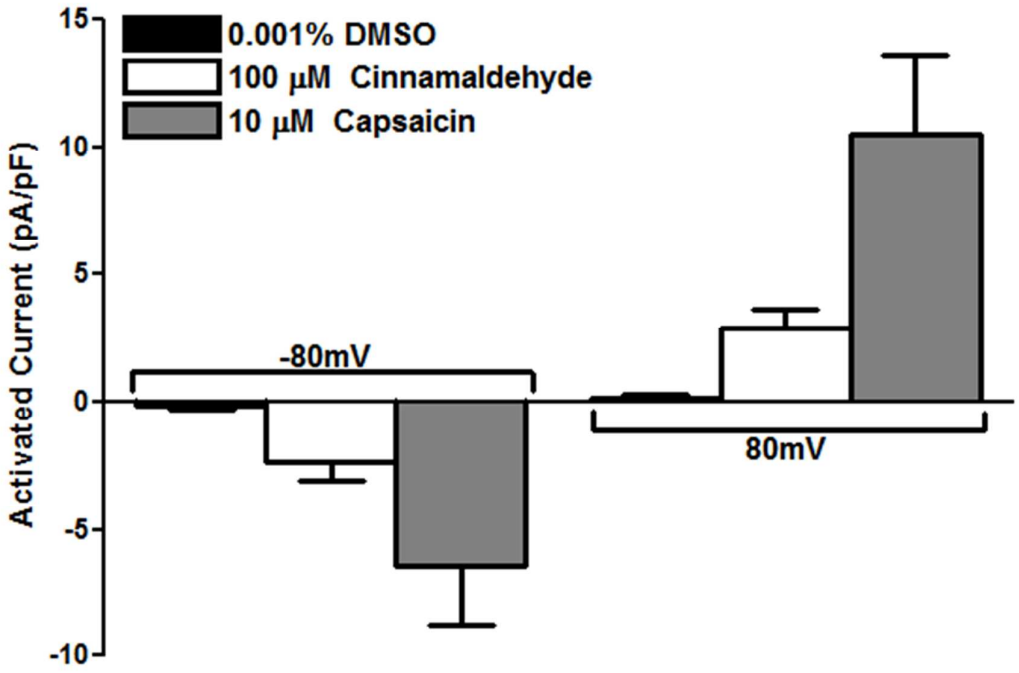
0.001% DMSO
100 µM Cinnamaldehyde
10 µM Capsaicin
Activated Current (pA/pF)
15
10
5
0
-5
-10
-80mV
80mV

Figure S3

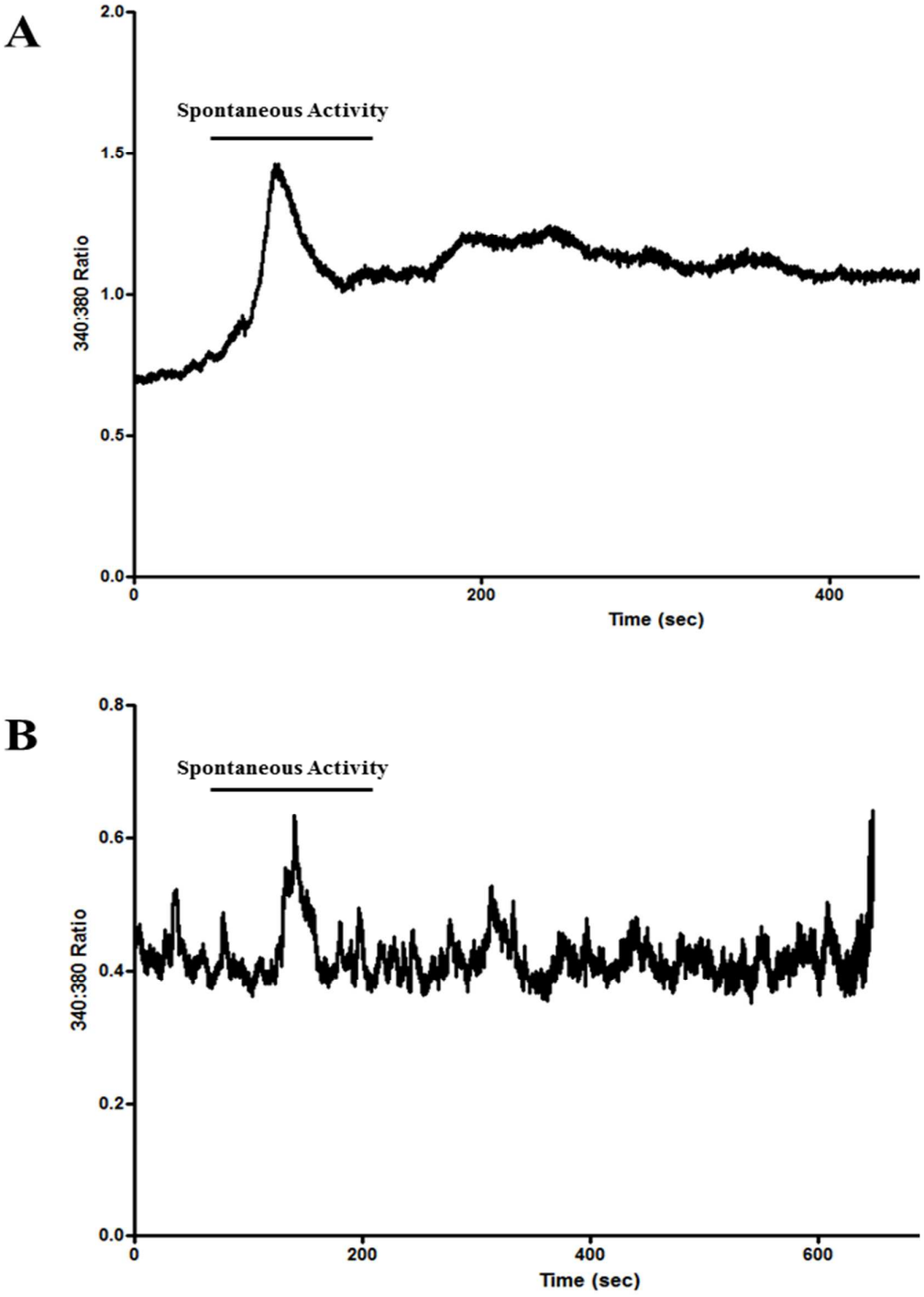
A
Spontaneous Activity
340:380 Ratio
2.0
1.5
1.0
0.5
0.0
0
200
400
Time (sec)
B
Spontaneous Activity
340:380 Ratio
0.8
0.6
0.4
0.2
0.0
0
200
400
600
Time (sec)

Figure S4

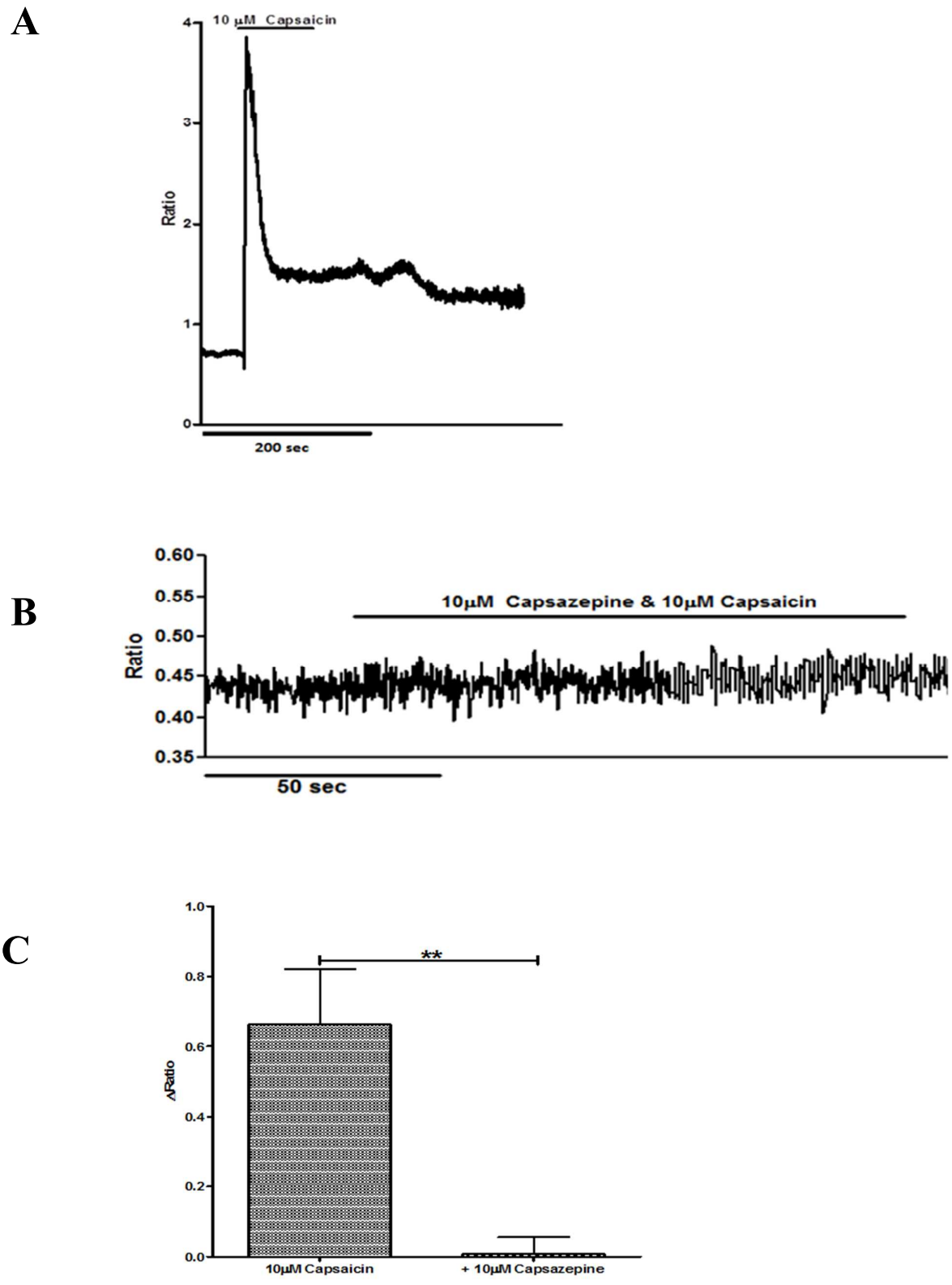
A
10 μM Capsaicin
Ratio
200 sec
B
10μM Capsazepine & 10μM Capsaicin
Ratio
50 sec
C
**
ΔRatio
10μM Capsaicin
+ 10μM Capsazepine

Figure S5

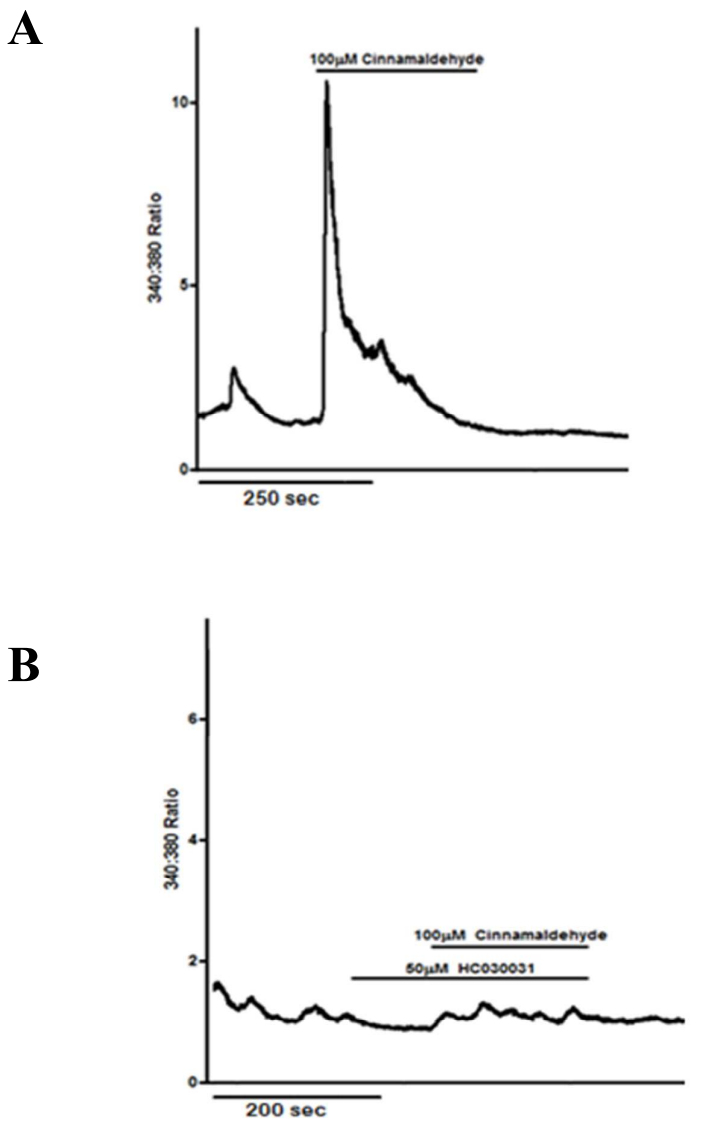
A
100μM Cinnamaldehyde
340:380 Ratio
10
5
0
250 sec
B
340:380 Ratio
6
4
2
0
100μM Cinnamaldehyde
50μM HC030031
200 sec
C
**
ΔRatio
10
8
6
4
2
0
100μM Cinnamaldehyde
+ 50μM HC030031

Figure S6

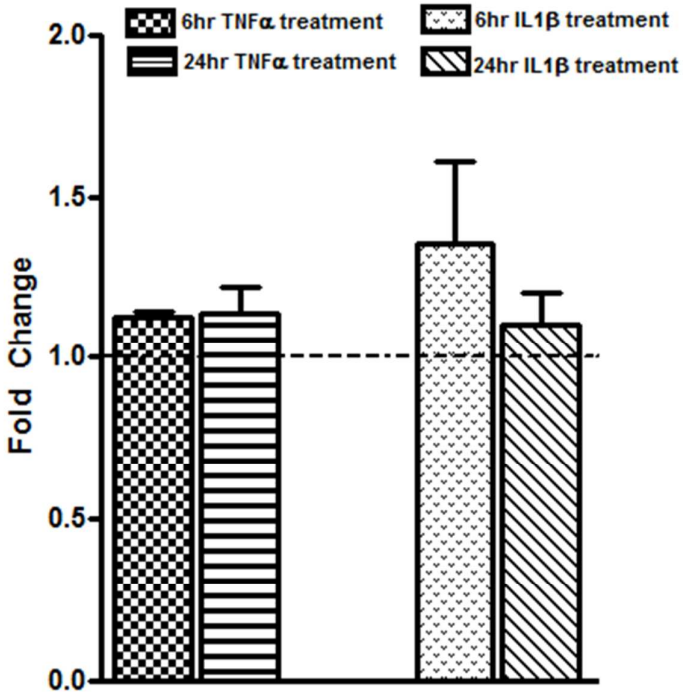
6hr TNFα treatment
6hr IL1β treatment
24hr TNFα treatment
24hr IL1β treatment
Fold Change
2.0
1.5
1.0
0.5
0.0

Figure S7

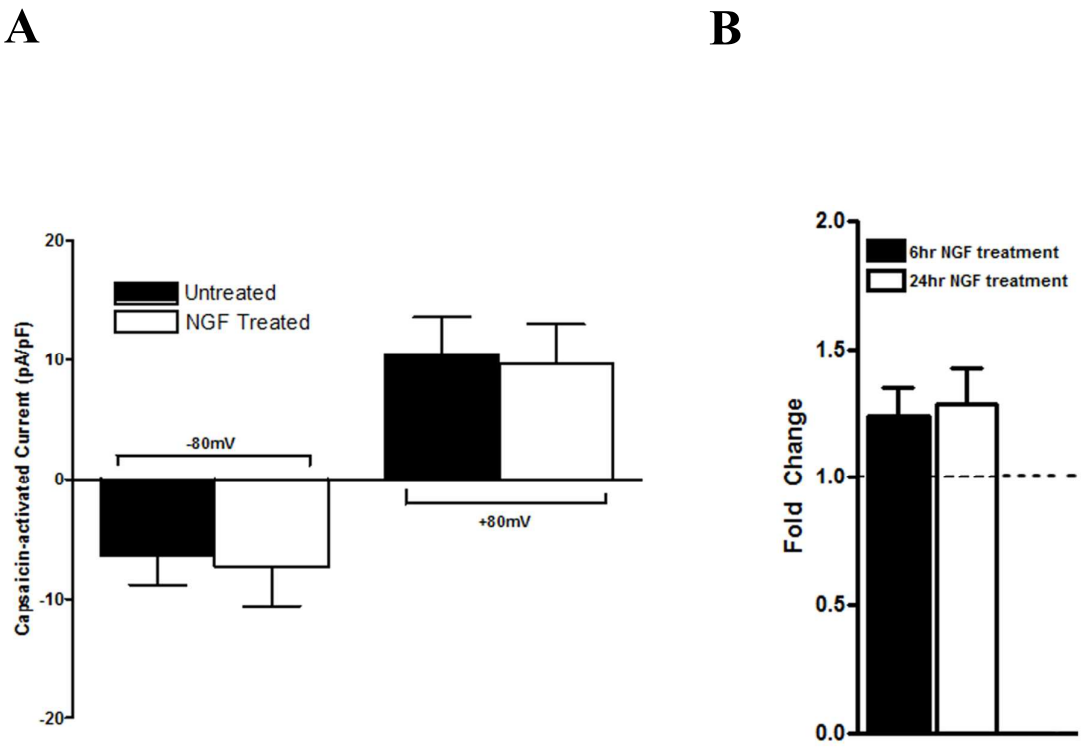
A
B
Untreated
NGF Treated
Capsaicin-activated Current (pA/pF)
20
10
0
-10
-20
-80mV
+80mV
6hr NGF treatment
24hr NGF treatment
Fold Change
2.0
1.5
1.0
0.5
0.0

Figure S8

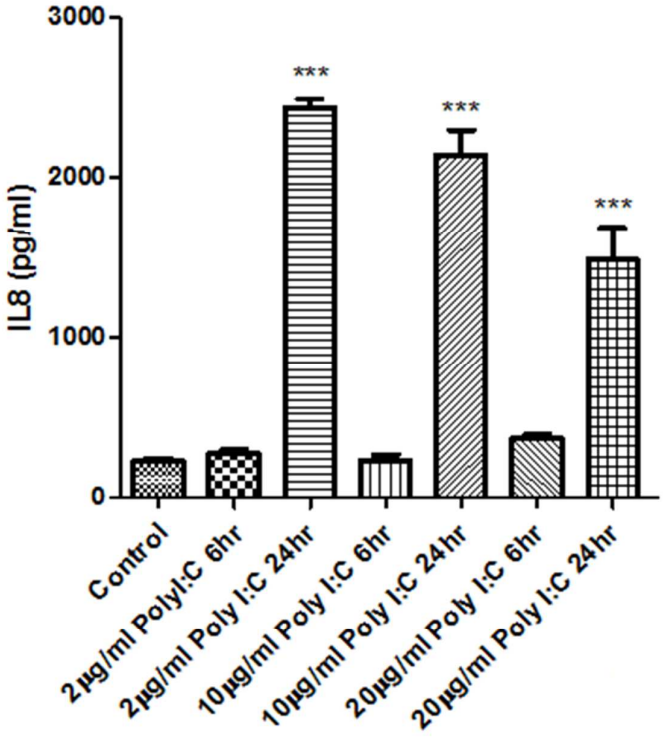
3000
2000
1000
0
IL8 (pg/ml)
***
***
***
Control
2µg/ml Poly I:C 6hr
2µg/ml Poly I:C 24hr
10µg/ml Poly I:C 6hr
10µg/ml Poly I:C 24hr
20µg/ml Poly I:C 6hr
20µg/ml Poly I:C 24hr

Figure S9